arXiv:2011.03121v1 [stat.ME] 5 Nov 2020

Hidden Markov Pólya trees for high-dimensional distributions

Naoki Awaya and Li Ma
Department of Statistical Science
Duke University, Durham, NC 27708, USA

September 3, 2022

Abstract

The Pólya tree (PT) process is a general-purpose Bayesian nonparametric model that has found wide application in a range of inference problems. The PT has a simple analytic form and the resulting posterior computation boils down to straight-forward beta-binomial conjugate updates along a partition tree over the sample space. Recent development in PT models shows that performance of these models can be substantially improved by (i) incorporating latent state variables that characterize local features of the underlying distributions and (ii) allowing the partition tree to adapt to the structure of the underlying distribution. Despite these advances, however, some important limitations of the PT that remain include—(i) the sensitivity in the posterior inference with respect to the choice of the partition points, and (ii) the lack of computational scalability to multivariate problems beyond a small number (< 10) of dimensions. We consider a modeling strategy for PT models that incorporates a very flexible prior on the partition tree along with latent states that can be first-order dependent (i.e., following a Markov process), and introduce a hybrid algorithm that combines sequential Monte Carlo (SMC) and recursive message passing for posterior inference that can readily accommodate PT models with or without latent states as well as flexible partition points in problems up to 100 dimensions. Moreover, we investigate the large sample properties of the tree structures and latent states under the posterior model. We carry out extensive numerical experiments in the context of density estimation and two-sample testing, which show that flexible partitioning can substantially improve the performance of PT models in both inference tasks. We demonstrate an application to a flow cytometry data set with 19 dimensions and over 200,000 observations.

1 Introduction

A Pólya tree (PT) process (Freedman, 1963; Ferguson, 1974; Lavine et al., 1992) is a stochastic process that generates random probability measures and is introduced as a prior for Bayesian nonparametric inference. While the PT generalizes the Dirichlet process (DP) (Ferguson, 1973) as it yields the DP under specific choices of hyperparameters (Ferguson, 1974), the statistical properties and thus practical applications of the PT are very different from those of the general DP. While the DP is most frequently used as a mixing distribution that induces latent clustering structures, the PT is often adopted when the underlying distribution is assumed to be absolutely continuous. Inference under the DP generally require Markov Chain Monte Carlo (MCMC) sampling, whereas that under the PT can often be done with exact conjugate updates.

The PT process is defined generatively on a recursive partition—or a partition tree—over the sample space through coarse-to-fine sequential probability assignment among tree nodes at each split of the tree. In a classical PT the tree is dyadic and the conditional probability assigned to the two sibling nodes at each tree split is given an independent beta prior. One of the most desirable features of the PT is its analytic simplicity and the ease in computing the posterior. Obtaining the posterior is straightforward from beta-binomial conjugacy and can be completed at a computational budget that scales linearly with the sample size.

The PT has been applied to various inference tasks beyond the original application of density estimation. A far-from-exhaustive list includes survival analysis (Muliere and Walker, 1997; Neath, 2003), imputing missing values (Paddock, 2002), goodness-of-fit tests (Berger and Guglielmi, 2001), two-sample comparison (Ma and Wong, 2011; Holmes et al., 2015; Chen and Hanson, 2014; Soriano and Ma, 2017), density regression Jara and Hanson (2011), ANOVA (Ma and Soriano, 2016), testing independence (Filippi et al., 2017), and hierarchical modeling (Christensen and Ma, 2019). The PT process has also been utilized in semi-parametric analyses such as in linear models (Walker et al., 1999; Hanson and Johnson, 2002) and generalized linear models (Walker and Mallick, 1997).

Early developments and applications of the PT are generally based on an *a priori* fixed partition tree on a univariate sample space. Many authors noted that the resulting inference can be highly sensitive to the choice of the partition points that define the tree, and in particular, the resulting process, both *a priori* and *a posteriori* can be very jumpy at the partition points. In the context of hypothesis testing and model choice, the sensitivity to the partition points is also reflected in the sometimes substantial change in the marginal likelihood/Bayes factor when the partition points are slightly varied. To remedy this issue, Paddock et al. (2003) modified the PT model so that all observations are generated from the PT model with slightly different

partition points. Hanson and Johnson (2002) and Hanson (2006) proposed a mixture of PTs by defining partition points along fixed quantiles of a parametric model and place a prior on the parametric model to allow inference on the partition points. This strategy does not allow individual partition points to be inferred from local features of the distribution but only the whole set of points according to the global structure of the distribution, and is most effective when the underlying density is close to the specified parametric model. Nieto-Barajas and Mueller (2012) took a different approach—instead of allowing the partition points to be more flexible, they modeled the probability assignments within each level of the tree in a correlated manner to smooth out the random measure over the boundaries of partitioning. While these approaches alleviate the sensitivity to partition points in the low-dimensional settings, they are not easily applicable (though in principle possible) to even just a handful of dimensions. Moreover, inference with these models generally require MCMC to sample from the posterior, whose effectiveness can (in fact often does) still suffer from the sensitivity with respect to the partition points.

Wong and Ma (2010) noted that in multivariate settings using an *a priori* fixed partition tree is extremely undesirable, and incorporating adaptivity into the partitioning strategy with respect to the structure of the underlying distribution is critical. They proposed to adopt a Bayesian CART-like recursive partitioning prior on the partition tree that allows optional stopping and selection on the dimension to divide at each tree split, leading to the so-called optional Pólya tree (OPT) model. Several follow-up works adopted this strategy into other inference tasks such as two-sample testing (Ma and Wong, 2011; Soriano and Ma, 2017) and density regression (Ma, 2013). However, in order to maintain the analytic simplicity of the resulting model and achieving MCMC-free exact Bayesian inference, the Bayesian CART-like prior has to be restricted to only divide at the middle point (or otherwise a pre-determined fixed point) on one of the dimensions on each tree split. Not only does this restriction hampers its ability to fully adapt to distributional structures, but it also makes the model suffer from the same sensitivity with respect to the choice of the partition points. Also, even with this restriction the resulting exact inference algorithm (based on recursive message passing) is only computationally practical for up to about 10 dimensions on continuous sample spaces.

In a different vein, recent development of the PT has demonstrated that in addition to improving the partition strategy, the statistical performance of these models can also be substantially improved by enriching the PT model with more flexible priors (than independent betas) on the probability assignment at each tree split (Jara and Hanson, 2011; Nieto-Barajas and Mueller, 2012; Ma, 2017). A powerful strategy for enriching the PT is by introducing latent state variables at each tree node and construct priors on the random conditional probabilities *given* these states to allow (i) more flexible regularization or shrinkage on these probability as-

signments (Ma, 2017) and (ii) borrowing of information across the sample space (Ma and Wong, 2011; Soriano and Ma, 2017) by incorporating dependency among the latent states among the tree nodes. A critical benefit of this latent variable model strategy is computational—when the latent state variables are modeled with Markov dependency, the analytical simplicity of the PT is maintained and exact Bayesian inference can proceed through an recursive message passing algorithm that maintains the same linear computational complexity as the standard PT with independent beta priors (Ma, 2017).

We are motivated by the following questions: Is it possible to incorporate into the PT a very flexible partition tree prior, such as the general Bayesian CART (i.e., without the restriction to partition at middle points), that will (i) enhance its adaptivity to distributional structures in multivariate settings; (ii) resolve its sensitivity to the choice of partition points; and (iii) allow a tractable form of the joint posterior and a posterior inference algorithm that is scalable to moderately high-dimensional problems (e.g., up to 100 dimensions)? Moreover, should such a strategy exist, can the resulting model and inference algorithm be compatible with incorporating (possibly dependent) latent states on the tree nodes?

The goals of making the partition tree prior more flexible while enhancing the computational scalability appear at odds with each other. Large tree spaces are well known to be very hard to compute over. In moderate to high dimensional settings exact inference involving flexible tree spaces is beyond reach and even the most advanced MCMC approaches tailor-made for trees encounter substantial difficulty due to the pervasive multi-modality of distributions in such spaces. Recent advances in sequential Monte Carlo (SMC) for regression tree models (Lakshminarayanan et al., 2013; Lu et al., 2013), however, suggest that efficient inference is possible in moderately high-dimensional settings (up to about 100 dimensions). Moreover, once the partition tree is sampled, the conditional posterior for the rest of the model can be computed analytically through recursive message passing. We will therefore exploit a hybrid strategy that uses a new SMC sampler to efficiently sample from the marginal posterior of the partition tree structure, and using recursive message passing to compute the exact conditional posterior of the latent state variables under Markov dependency. To illustrate its versatility, we will demonstrate our inference algorithm in multivariate settings for both density estimation and two-sample comparison.

Beyond the methodological development, we will also investigate the theoretical properties of the posterior on the partition tree and the latent states. Previous theoretical literature on the PT and related models have mostly focused on establishing the posterior consistency and contraction rate of the random measure induced under these models. In multivariate settings, however, the underlying tree structure itself is highly, if not most, informative about the underlying distribution. Moreover, in problems involving model choice and hypothesis

testing, it is often the latent states that are most relevant for inference. As such, we instead focus on analyzing the asymptotic behavior of the marginal posterior on the partition tree and that on the latent states, establishing consistency results on their convergence toward the trees and states that the most closely characterize the underlying truth.

The rest of the paper is organized as follows. In Section 2 we describe a flexible prior on the partition tree structure that relaxes the restriction of "dividing in the middle" on partition points and present a general form of PT models that adopt this prior along with latent states associated with the tree nodes with a Markov dependency structure. In Section 3, we present our hybrid computational strategy that can work effectively up to 100 dimensions consisting of an SMC algorithm for sampling on the marginal posterior of the partition tree and a recursive message passing algorithm for obtaining the exact conditional posterior of the latent states and the predictive distribution given the sampled trees. In Section 4 we investigate the asymptotic properties of the tree structures and latent states identified under the posterior model. In Section 5, we carry out extensive numerical experiments to examine the performance of our method in the context of two important applications of PTs—density estimation and the two-sample problem. In Section 7 we conclude with a brief discussion.

2 Method

In this section, we first review the original PT process (Ferguson, 1973; Lavine et al., 1992) in Section 2.1. Then we introduce a new flexible prior for tree structures in Section 2.2 and provide a general framework of PT models with both the flexible partition prior and latent states under a Markov dependency in Section 2.3.

2.1 Pólya trees

Without loss of generality, we consider a continuous sample space represented as a d-dimensional rectangle $\Omega = (0, 1]^d$. We use μ to denote the Lebesgue measure on Ω. A (dyadic) recursive partitioning T on Ω is a sequence of partitions of Ω such that the partition blocks at each level of the partitioning are obtained by dividing each block in the previous level into two children blocks. Formally, we can write $T = \bigcup_{k=0}^{\infty} \mathcal{A}^k$, where $\mathcal{A}^k$ is a partition of Ω in the kth level. More specifically, $\mathcal{A}^0 = \{\Omega\}$, and $A \in \mathcal{A}^k$ $(k = 1, 2, \dots)$ is divided into A_l and A_r, which satisfy $A_l, A_r \in \mathcal{A}^{k+1}$, $A_l \cup A_r = A$, and $A_l \cap A_r = \emptyset$. (Throughout the discussion, a subscript l or r to a node indicates the left or right child node.) For example, in the original PT, $d = 1$ and the tree is recursively divided at the middle point of each node, and so nodes in level k are of the form $(l/2^k, (l + 1)/2^k]$ for some $l \in 0, \dots, 2^k - 1$. Another common strategy is to

define the tree based on the quantiles of a probability measure F so that $A \in \mathcal{A}^k$ is of the form $A = (F^{-1}(\frac{l}{2^k}), F^{-1}(\frac{l+1}{2^k})]$ for $l \in 0, \ldots, 2^k - 1$.

Many authors have opted to use a sequence of binary indicators to index each node in the dyadic tree T. For example, to denote a node in the kth level, we often use $\boldsymbol{\epsilon} = \epsilon_1 \cdots \epsilon_k$, where for $i = 1, 2, \ldots$, $\epsilon_i = 0$ means the "left" branch and $\epsilon_i = 1$ the "right". This notation based on a path to reach the node from the root node works to uniquely indicate a node when the tree structure is fixed. When the partition tree T is assumed to be an unknown quantity, the binary sequence does not by itself pin down a region in Ω—two nodes with the same index $\boldsymbol{\epsilon}$ can be different when they belong to two different trees. On the other hand, the alternative notation that uses the combination of $(T, \boldsymbol{\epsilon})$ to index nodes is not only cumbersome, but more importantly it hides the useful fact that a region in Ω might be a node in many different trees (though indexed differently under each), which will have important implication in the computational implementation of such models. In particular, many quantities to compute can be associated with the nodes rather than the trees to avoid massive amounts repetitive computation. Hence, we shall directly use a set notation $A \subset \Omega$ to directly index a node A in T.

Given a partition tree T, we can define a random measure Q by putting a prior on the conditional probability $\theta(A) = Q(A_l \mid A) = 1 - Q(A_r \mid A)$ at each $A \in T$. Under the original PT model, the parameters $\theta(A)$ follow independent beta distributions $Beta(\alpha_l(A), \alpha_r(A))$, where $\alpha_l(A)$ and $\alpha_r(A)$ are hyper-parameters. Under independent beta priors, the posterior has a simple conjugate form given an i.i.d. sample $x_1, \ldots, x_n$ from Q:

$$P(\theta(A) \mid x_1, \ldots, x_n) = P(\theta(A) \mid n(A_l), n(A_r)) = Beta(\theta \mid \alpha_l(A) + n(A_l), \alpha_r(A) + n(A_r)),$$

where $n(A)$ represents the number of observations in a set $A \subset \Omega$. Though the tree is infinitely deep to ensure full support of the PT, for practical purposes, one can set a sufficiently large maximum depth (or resolution) of T and compute the posteriors of $\theta(A)$'s defined on this finite tree structure (Hanson and Johnson, 2002). We shall refer to a node in the deepest level as a "leaf" or "terminal node". On a leaf, the conditional distribution can be set to a baseline, such as the uniform distribution $\mu(\cdot \mid A)$. In Section 3 when we present inference algorithms, we shall adopt this practical strategy and assume T is finite and use $\mathcal{N}(T)$ and $\mathcal{L}(T)$ to denote the collection of the non-terminal nodes and the leaf nodes, respectively. For the rest of the current Section which describes our prior model, this assumption is not particularly important.

2.2 Incorporating flexible partition points

In classical PTs the tree structure is fixed—that is, the way each node A can be further divided into A_l and A_r is *unique* and *a priori* given, and the model is specified only in terms of the

conditional probability assignment among the pre-determined nodes. However, as described in Section 1, in multivariate problems, it is critical allow more flexible partition trees that can adapt to the underlying structure of the distribution.

Hence, we incorporate a prior on T by randomizing both the dimension in which to divide a node and the location along that dimension to divide. Suppose we have a node A written in the following rectangle form:

$$A = (a_1, b_1] \times \cdots \times (a_d, b_d].$$

We consider a Bayesian CART-like prior that divides A into two rectangular children by cutting along a randomly chosen dimension at a random location. The dimension to divide $D(A) \in \{1, 2, \ldots, d\}$, and the (relative) location to divide $L(A) \in (0, 1)$ are given independent priors of the following forms:

$$D(A) \sim \text{Multi}(\lambda_1(A), \ldots, \lambda_d(A)) \quad \text{and} \quad L(A) \sim \sum_{l=1}^{N_L-1} \beta_l(A)\delta_{l/N_L}(\cdot), \tag{1}$$

where $\delta_x(\cdot)$ represents the unit point mass at x, both $\lambda_i(A)$'s and $\{\beta_l(A)\}_{l=1,\ldots,N_L-1}$ sum is 1, and N_L-1 is the total number of grid points along $(0, 1)$. In the above, we have adopted an even grid over (0,1) but it does not have to be as such. Also note that in principle we could adopt a continuous prior for $L(A)$. A discretized prior is preferable however because it simplifies posterior computation. In practice, as long as the grid is dense enough, the discrete prior will be practically just as flexible. Indeed we have verified in extensive numerical experiments that when N_L is large enough (more than 30 to 50) over a uniform grid, posterior inference no longer improves in any noticeable way.

With $D(A) = j$ and $L(A) = l/N_L$, the two children nodes A_l and A_r are

$$A_l = (a_1, b_1] \times \cdots \times (a_j, a_j + l/N_L \cdot (b_j - a_j)] \times \cdots \times (a_d, b_d],$$
$$A_r = (a_1, b_1] \times \cdots \times (a_j + l/N_L \cdot (b_j - a_j), b_j] \times \cdots \times (a_d, b_d].$$

The new prior can be regarded as a generalization of a prior in the OPT model (Wong and Ma, 2010) in that the OPT's tree prior can be written with $D(A)$ and $L(A)$ but $L(A)$ is always fixed to a single grid point such as 1/2. Figure 1 illustrates the random partitioning in 2D.

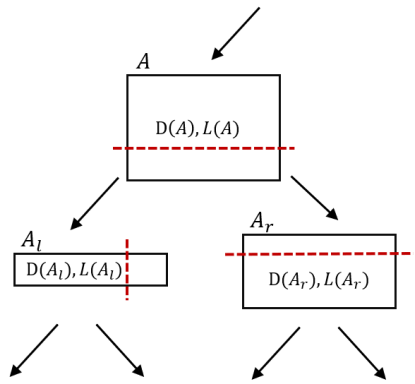

Figure 1: A graphical representation of the recursive process to generate a tree.

For the prior on $D(A)$, we set $\lambda_j(A) = 1/d$ for all nodes A as a default choice. For the prior on $L(A)$, extensive numerical experiments indicate that when $L(A)$ is given a weak prior widely spread over $(0, 1)$, the resulting inference can be sensitive to the "tail" behaviors of the distribution in the node as sample size grows, resulting in posteriors of $L(A)$ concentrated near the extreme values 0 and 1. This issue can be effectively addressed by making the prior of $L(A)$ depends on the sample size $n(A)$ so that it encourages more balanced divisions at large sample sizes. More specifically, as our Lemma C.2 in Section 4 suggests, the likelihood grows in the the order of $\exp(n(A))$, and so we need an exponentially decaying tail for the prior to counter the sensitivity in the tails. As such we adopt the following prior

$$P(L(A) = l/N_L = \beta_l \propto \exp\left[-\eta n(A) f(|l/N_L - 0.5|)\right], \; l = 1, \ldots, N_L - 1, \tag{2}$$

where η is a hyper-parameter and f is a monotonically increasing function. In the following, we shall use a function $f(x) = x$, and so our prior on $L(A)$ is essentially a (discretized) Laplace distribution.

Another generalization of the prior on $L(A)$ is to incorporate a spike-and-slab set-up that incorporates a spike at the middle point 1/2. In particular, one can adopt a dependent spike prior among the nodes such that once a node A is divided exactly at the middle point, so are its descendants. This generalization is particularly helpful computationally as it will substantially reduces the amount of computation in our sequential Monte Carlo algorithm in regions of the sample space where the data are either sparse or lacking interesting structure, e.g., close to the uniform distribution. We implements the spike-and-slab in our software but defer the details of this generalization to the Appendix to avoid distracting the reader from the main ideas.

Given the tree prior, our PT model now consists of the two components—tree generation and conditional probability assignment. Figures 2(a) and 2(b) present a graphical model representation for each.

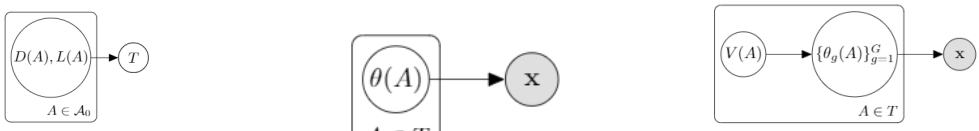

(a) PT process ($\mathcal{A}_0$: All potential nodes)

(b) PT process

(c) Generalized PT process with latent states

Figure 2: Graphical representation of PT models given the tree T. The hyper-parameters are hidden for simplicity.

2.3 Hidden Markov Pólya tree models

2.3.1 General framework

Next, we will extend the above model to accommodate two recent developments in the PT literature: (i) jointly modeling of multiple samples; and (ii) incorporating latent state variables along the tree structure. The first extension enables us to analyze data sets with multiple samples such as in two-sample comparison and hierarchical modeling, while the second enriches the flexibility of the model to more realistically characterize distributional features. As in recent literature, we consider incorporating discrete state variables that follow a hidden Markov process on the tree structure. All description in this section pertains to the model given the randomly generated partition tree T, and so to avoid repetitiveness we shall not keep stating "given T".

Let $\mathbf{Q} = \{Q_g\}_{g=1}^G$ denote a set of G random measures. Given $\mathbf{Q}$, the observations $x_g = (x_{g,1}, \ldots, x_{g,n_g})$ for $g = 1, \ldots, G$ are independently generated as i.i.d. samples from Q_g. The collection of all observations are denoted by $\mathbf{x} = \{x_g\}_{g=1}^G$.

Next we specify a prior on $\mathbf{Q}$ in terms of a joint prior on the conditional probability on each $A \in T$,

$$\theta_g(A) = Q_g(A_l \mid A) = 1 - Q_g(A_r \mid A).$$

Instead of modeling the $\theta_g(A)$'s by independent priors, we use latent variable modeling to incorporate dependency among the tree nodes. Specifically, we let $\{V(A) : A \in T\}$ denote a collection of latent state variables, one for each A, and without loss of generality, assume that $V(A)$ takes discrete values from $\{1, \ldots, I\}$. (In practice, the number of states can differ among A.) Joint priors of $\theta_g(A)$ for all g and A are then defined conditional on these latent states.

Existing literature has exploited these latent states to characterize both the structure of each distribution Q_g (the within-sample structure) and the relationship among the Q_g (the between-sample structures). An example of within-sample structures is the smoothness of the

underlying distribution, which is explored in the context of density estimation (Ma, 2017). Examples of between-sample structures include whether two (or more) distributions are different or not (Soriano and Ma, 2017) as well as the components of cross-sample variance (Christensen, 2017).

Dependent modeling of the latent states over the partition tree is desirable as *a priori* one would expect interesting structures (both within-sample and between-sample) to exhibit themselves in a correlated manner over the sample space—e.g., functions tend have similar smoothness over adjacent locations, and two-sample difference tend to be clustered in space. A powerful and computational efficient strategy for modeling such dependency over the tree is by a hidden Markov process along the tree (Crouse and Baraniuk, 1997; Ma and Soriano, 2018), which starts from the root of the partition tree, ω, and sequentially generates the latent states in a coarse-to-fine fashion according to (possibly node-specific) transition matrices $\boldsymbol{\xi}(A)$ whose (i, i')th element is

$$\boldsymbol{\xi}(A)_{i,i'} = P(V(A) = i' \mid V(A^p) = i) \quad \text{for } i, i' \in \{1, \ldots, I\},$$

where A^p is A's parent. (We shall use superscript "p" to indicate the parent of a node in T.)

Given the $V(A)$'s, $\{\theta_g(A)\}_{g=1,\ldots,G}$ are then modeled independently. The specific choices of these conditional priors are problem-dependent. We will give two examples below. Figure 2(c) presents a graphical model representation for the latent state modeling on a PT given T, which along with our generalized prior on the partition tree T presented in Figure 2(a) forms the most general version of the model we consider in this work.

Example 1: Density estimation with adaptive smoothness

An example in which the latent state $V(A)$ characterizes within-sample structures is density estimation on a single sample. In the case the number of groups G is 1 and a parameter $\theta_1(A)$ $(A \in T)$ can follow the beta distribution given the latent state. This beta prior is here written in the form of $Beta(m(A)\nu(A), (1 - m(A))\nu(A))$, where $m(A)$ is the prior mean, which characterizes the "center" of the random measure, and $\nu(A)$ is the precision parameter that characterizes the prior smoothness of the random measure. Ma (2017) proposed the adaptive Pólya tree (APT) model which incorporates latent states to allow different levels of local smoothness in the underlying distribution. This is achieved by specifying a conditional prior on the precision parameter

$$\nu(A) \mid V(A) = i \sim F_i$$

where the conditional prior F_i given $V(A)$ is assumed to be in a stochastic order corresponding to increasing smoothness $F_1 \prec F_2 \prec \cdots \prec F_I$.

Example 2: Two-sample problem

In two-sample comparison, we are interested testing and identifying differences between two measures $\mathbf{Q} = \{Q_g\}_{g=1,2}$ based on an i.i.d. sample from each. The "global" testing problem can be formulated as testing the following null and alternative hypotheses:

$$H_0 : Q_1 = Q_2 \quad \text{vs} \quad H_1 : Q_1 \neq Q_2.$$

Noting that two-sample differences may exist in parts of the sample space and not others, the coupling OPT (Ma and Wong, 2011) and the multi-resolution scanning (MRS) model (Soriano and Ma, 2017) are PT-based models for a pair of random measures that allow the measures to differ on some nodes $A \in T$ and not others. This more "local" persective on the two-sample problem enables these models to not only test for H_0 vs H_1, but to identify regions on which the two measures differ. To achieve this, these models incorporate a state variable that characterizes whether the conditional probabilities on each A are equal between the two measures:

$$V(A) = 1 \Leftrightarrow Q_1(A_l \mid A) \neq Q_2(A_l \mid A), \tag{3}$$

$$V(A) = 2 \Leftrightarrow Q_1(A_l \mid A) = Q_2(A_l \mid A). \tag{4}$$

When $V(A) = 1$, $\theta_1(A)$ and $\theta_2(A)$ are given independent beta priors, whereas if $V(A) = 2$, $\theta_1(A) = \theta_2(A)$ and is generated from a single beta prior. Markov dependency among the states on different nodes can then be incorporated to induce the desired spatial correlation of cross-sample differences. Additional latent states can be further incorporated to reflect more complex relationships between the distributions and to enhance the performance of the model. In fact, the MRS also incorporates an additional state $V(A) = 3$, which introduces the same coupled prior as $V(A) = 2$, but works as an absorbing state in the Markov process so that once $V(A) = 3$, all descendants of A will remain in that state, corresponding to the case that the two conditional distributions $Q_1(\cdot|A)$, and $Q_2(\cdot|A)$ are completely equal.

3 Bayesian inference

In sum, our model consists of the following components: (i) the partition tree T defined by the dimension and location variables D's and L's, which follow the priors given in Eq. (1); (ii) the latent state variables $V(A)$ given T which follow a Markov prior; (iii) the conditional probabilities along the given tree T, $\{\theta_g(A)\}_{g=1}^G$, whose prior given the latent states are independent betas that can be problem-specific; and finally (iv) given the random measures Q_g defined by T and $\theta_g(A)$'s, we observe an i.i.d. sample $\boldsymbol{x}_g$ from each Q_g, independently across g. Formally,

we have the following full hierarchical model:

$$
\begin{aligned}
T \mid \boldsymbol{\lambda}, \eta &\sim p(T \mid \boldsymbol{\lambda}, \eta) \\
\{V(A) : A \in T\} \mid \boldsymbol{\xi}, T &\sim \text{Markov}(\boldsymbol{\xi}) \\
(\theta_1(A), \ldots, \theta_g(A)) \mid V(A), T &\overset{\text{ind}}{\sim} p(\theta_1(A), \ldots, \theta_G(A) \mid V(A)) \text{ for } A \in T \\
\boldsymbol{x}_g = (x_{g,1}, x_{g,2}, \ldots, x_{g,n_g}) \mid Q_g &\overset{\text{iid}}{\sim} Q_g \text{ for } g = 1, 2, \ldots, G.
\end{aligned}
$$

The key to Bayesian inference is the ability to either compute or sample from the joint posterior $(T, \mathbf{V}, \boldsymbol{\theta})$ given all data $\boldsymbol{x} = (\boldsymbol{x}_1, \ldots, \boldsymbol{x}_G)$, where $\mathbf{V}$ and $\boldsymbol{\theta}$ represent the totality of all latent states and conditional probabilities given T respectively. While in some problems such as density estimation one may mainly be interested in just the marginal posterior of the Q_g's, in others such as two-sample comparison where one want to characterize the between-sample relationships among the distributions, the latent states (along with T) are often of prime interest. In multivariate and even high-dimensional problems, the tree structure T is also of great interest as it always sheds light on the underlying (within-sample and between-sample) structures in the distributions. As such, in the following we aim to draw samples from the full joint posterior, and do so in such a way that is scalable to moderately high-dimensional problems (e.g., 100 dimensions), which according to our knowledge is not achievable by any existing inference algorithms for PT-based models even with fixed partition points and no latent states.

To this end, we shall take advantage of recent development in both sequential Monte Carlo (SMC) sampling tree-based Bayesian models (Lakshminarayanan et al., 2013; Lu et al., 2013) and advances in message passing algorithms for PT models with hidden Markov structures in low-dimensional settings (Ma, 2017). We next propose a hybrid algorithm that combines these two computational strategies to effectively sample from the joint posterior in high-dimensional spaces in two stages:

1. **Sampling from the marginal posterior of the partition tree**

   We design an SMC sampler—that is, a particle filter—to sample a collection of tree structures $T^1, \ldots, T^M$ by growing each tree from coarse to fine scales. It uses proposals based on one-step look-ahead message passing to construct proposal distributions for $D(A)$ and $L(A)$, one node at a time.

2. **Exact computing of the conditional posteriors of V and θ given the sampled trees**

   Given each tree sampled by the SMC, we analytically compute the exact conditional posteriors of $V(A)$'s and $\theta(A)$'s using recursive message passing, a form of dynamic programming.

Next we describe the two stages of the computation scheme in details.

3.1 SMC to sample from tree posterior

In the SMC stage to sample the trees, each particle stores a realized form of a finite tree structure, and one node of each tree is divided at each step of the algorithm. A finite tree we obtain by dividing the sample space t times is denoted by T_t, and for this tree we define the target distribution

$$\pi_t(T_t) = P(T_t \mid \mathbf{x}) \propto P(T_t)P(\mathbf{x} \mid T_t).$$

In this definition, $P(T_t)$ is the joint prior of the variables $D(A)$'s and $L(A)$'s for the non-leaf nodes of T_t, and $P(\mathbf{x} \mid T_t)$ is the likelihood defined by the hierarchical model, in which $\mathbf{V}$ and $\boldsymbol{\theta}$ are integrated out. To sample from this target distribution, we sequentially construct a set of M particles $\{T_t^m, W_t^m\}_{m=1}^M$, where T_t^m is a realized tree and W_t^m is the associated importance weight. An example of the generated tree structures is presented in Figure 3. In this example, the sample space has been divided three times, and in the next step, new partition boundaries are added in gray colored nodes. Following Lakshminarayanan et al. (2013), we adopt a breadth-first tree-growth strategy by dividing the oldest leaf node—that is, the one generated in the earliest step—in each step. Each node is segmented by a boundary whose direction and location are randomly drawn from a proposal distribution, so a finite tree T_t is formed by a sequence of decisions $\{J_s\}_{s=1}^t$, where $J_s = (D_s, L_s)$ correspond to the variables D and L, respectively. Hence, at the tth step of the SMC, we want to generate values of J_t to approximate $\pi_t(T_t)$ given T_{t-1}.

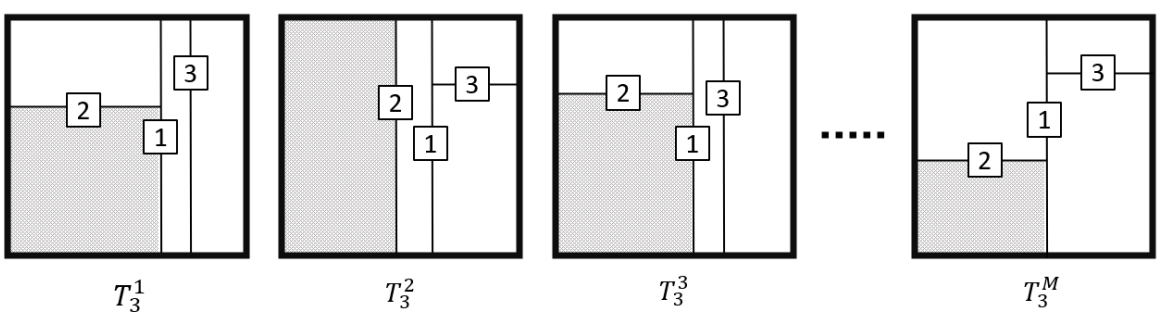

Figure 3: An example of realized finite trees in the particle system. The numbers in the squares indicate in which step the boundaries are drawn. The nodes colored gray are divided in the next step.

We propose the value of J_t from the conditional posterior $\pi_t(J_t \mid T_{t-1})$, that is, the posterior of J_t given that the current tree if T_{t-1} and only one more node can be added. This

is effectively a one-step look-ahead approximation to the conditional posterior of the full tree given T_{t-1}, and it can be computed at each step with constant computational cost with complexity $O(N_L dn(A_t))$, where $A_t \in T_{t-1}$ is the current node divided at the tth step. As such, our inference algorithm scales linearly in both the dimensionality and the sample size.

To see how exactly this proposal is computed, we consider the situation where we aim to divide the current node $A_t \in T_{t-1}$ into $A_{t,l}$ and $A_{t,r}$ with decision J_t. In generating J_t from $\pi_t(J_t \mid T_{t-1})$, we compute the following two quantities.

First, for every possible decision J_t and state $i = 1, \ldots, I$, we compute the marginal likelihood $M_i(A_t \mid J_t)$ on a node A_t under that decision, which is

$$M_i(A_t \mid J_t) = \int \left\{ \prod_{g=1}^{G} \theta_g(A_t)^{n_g(A_{t,l})} (1 - \theta_g(A_t))^{n_g(A_{t,r})} \right\} dP(\theta_1(A_t), \ldots, \theta_G(A_t) \mid V(A_t) = i), \tag{5}$$

where $n_g(A)$ denote the number of observations of the gth group included in A. For example, if the number of groups G is 1 and a parameter $\theta_1(A)$ follows the beta prior written as $Beta(\alpha_l^i(A), \alpha_r^i(A))$ when $V(A) = i$, then the marginal likelihood has the following expression

$$M_i(A \mid J_t) = \frac{B(\alpha_l^i(A) + n_1(A_l), \alpha_r^i(A) + n_1(A_r))}{B(\alpha_l^i(A), \alpha_r^i(A))},$$

where $B(\cdot, \cdot)$ is the beta function.

Second, given the decision J_t, for every state $i = 1, \ldots, I$, we define a function $\varphi_i(A_t)$ as follows:

$$\boldsymbol{\varphi}_i(A_t) = \begin{cases} \frac{\boldsymbol{\xi}_{1,i}(\Omega) M_i(\Omega|J_t)}{\sum_{j=1}^{I} \boldsymbol{\xi}_{1,j}(\Omega) M_j(\Omega|J_t)} & (A_t = \Omega) \\ \frac{\sum_{j=1}^{I} \varphi_j(A_t^p) \boldsymbol{\xi}_{j,i}(A_t) M_i(A_t|J_t)}{\sum_{k=1}^{I} \sum_{j=1}^{I} \varphi_j(A_t^p) \boldsymbol{\xi}_{j,k}(A_t) M_i(A_t|J_t)} & (\text{Otherwise}), \end{cases} \tag{6}$$

where A_t^p is A_t's parent node. This function is recursive in the sense that its value on A_t depends on that on the parent of A_t. Note that this function can always be computed at each step t because $\varphi_j(A_t^p)$ has been computed in step $t-1$. (Lemma C.1 in the supplementary materials shows that $\boldsymbol{\varphi}_i(A_t)$ is exactly the posterior probability of $V(A_t) = i$ given the tree T_t.)

With these quantities, we can establish the relationship between $\pi_{t-1}(T_{t-1})$ and $\pi_t(T_t)$, from which we can obtain the SMC algorithm, as shown in the following proposition.

Proposition 3.1. *Let $h(J_t \mid A_t)$ be a function of J_t defined as*

$$h(J_t \mid A_t) = \sum_{i=1}^{I} \left\{ \sum_{j=1}^{I} \boldsymbol{\varphi}_j(A_t^p) \boldsymbol{\xi}_{j,i}(A_t) \right\} M_i(A_t \mid J_t) \frac{\mu(\mathbf{x}(A_{t,l}) \mid A_{t,l}) \mu(\mathbf{x}(A_{t,r}) \mid A_{t,r})}{\mu(\mathbf{x}(A_t) \mid A_t)}. \tag{7}$$

Then the target distribution $\pi_t(T_t)$ can be expressed in terms of $\pi_{t-1}(T_{t-1})$ as

$$\pi_t(T_t) = C\pi_t(T_{t-1})\pi_t(J_t \mid T_{t-1})w_t(T_{t-1}),$$

where C is a constant and

$$\pi_t(J_t \mid T_{t-1}) = \frac{P(J_t)h(J_t \mid A_t)}{\sum_{j_t} P(j_t)h(j_t \mid A_t)},\ w_t(T_{t-1}) = \sum_{j_t} P(j_t)h(j_t \mid A_t).$$

The summation over j_t is taken over all possible decisions.

To sample from the conditional posterior $\pi_t(J_t \mid T_{t-1})$, a natural choice is to sample from the marginal $\pi_t(D_t \mid T_{t-1})$ and then sample from $\pi_t(L_t \mid D_t, T_{t-1})$. From Proposition 3.1, $\pi_t(D_t \mid T_{t-1})$ is $Multi(\tilde{\lambda}_1(A_t), \ldots, \tilde{\lambda}_d(A_t))$, where

$$\tilde{\lambda}_j(A_t) \propto \sum_{l=1}^{N_L-1} \pi_t((j, l/N_L) \mid T_{t-1}) \propto \lambda_j(A_t) \sum_{l=1}^{N_L-1} \beta_l(A_t)h((j, l/N_L) \mid A_t)$$

and, given $D(A_t) = j$, the conditional posterior of $L(A_t)$ for $l = 1, \ldots, N_L - 1$ is

$$\pi_t(L_t = l/N_L \mid D_t = j, T_{t-1}) = \sum_{l=1}^{N_L-1} \tilde{\beta}_l(A_t)\delta_{l/N_L}(\cdot),$$

where

$$\tilde{\beta}_l(A_t) \propto \beta(A_t)h(j, l/N_L \mid T_{t-1}).$$

After generating the values of D_t and L_t, we compute the incremental weight

$$w_t(T_{t-1}) = \sum_{j=1}^{d} \sum_{l=1}^{N_L-1} \lambda_j(A_t)\beta_l(A_t)h((j, l/N_L) \mid A_t),$$

with which we update the importance weight W_t from W_{t-1} as

$$W_t \propto W_{t-1}w_t(T_{t-1}).$$

The incremental weight $w_t(T_{t-1})$ can be interpreted as a component that evaluates how beneficial dividing A_t is.

We stop dividing A_t if either (i) the depth of A_t is equal to a pre-set maximum resolution K or (ii) the number of observations in A_t is less than some threshold (e.g., 5). The SMC algorithm is terminated when all the nodes of all the particles are no longer divided.

A common technique in SMC is to resample the particles according to the importance weights $\{W_t^m\}_{m=1}^M$ when the effective sample size of the particles drops below a level. In

sampling from tree space distributions, however, the importance weights are affected by the choice of nodes to divide in multiple steps, and so the standard resampling scheme can be too "short-sighted" and often results in sacrificing promising trees prematurely. To address this issue we follow the strategy proposed in Lu et al. (2013) by resampling the particles according to weights $a_t^m \propto (W_t^m)^\kappa$ for some $\kappa \in (0, 1]$, and compute the new importance weights proportional to W_t^m/a_t^m. We generally recommend using a moderate choice of κ such as 0.5, which we have found to be satisfactory in a variety of numerical experiments, and will be our default choice in all of our later examples.

We summarize the SMC algorithm in updating the particle system from $\{T_{t-1}^m, W_{t-1}^m\}_{m=1}^M$ to $\{T_t^m, W_t^m\}_{m=1}^M$ below in pseudo-code form. All operations involving the index m is repeated for $m = 1, \ldots, M$.

---

1. Choosing the current node

From T_{t-1}^m, choose the oldest node from the current leafs, which is denoted by A_t.

2. Obtaining the information of the parent node

Locate A_t's parent node, A_t^p, and fetch the values of $\boldsymbol{\varphi}_i(A_t^p)$ for $i = 1, \ldots, I$.

3. Computing the necessary quantities

For all possible decisions $J_t = (D_t, L_t)$, compute $M_i(A \mid J_t)$ $(i = 1, \ldots, I)$ and $h(J_t \mid A_t)$.

4. Dividing the current node

Compute the parameters $\tilde{\lambda}_j(A_t)$ for $j = 1, \ldots, d$ and sample

$$D_t^m \sim Multi(\tilde{\lambda}_1(A_t), \ldots, \tilde{\lambda}_d(A_t)).$$

Given D_t^m, compute the parameters $\tilde{\beta}_l(A_t)$ for $l = 1, \ldots, N_L - 1$ and sample

$$L_t^m \sim \sum_{l=1}^{N_L-1} \tilde{\beta}_l(A_t)\delta_{l/N_L}(\cdot).$$

Divide the current node A_t with $J_t^m = (D_t^m, L_t^m)$ to obtain the updated tree T_t^m.

5. Updating the importance weight

Compute the incremental weight $w_t(T_{t-1}^m)$ and update the importance weights as

$$W_t^m = \frac{W_{t-1}^m w_t(T_{t-1}^m)}{\sum_{m'=1}^M W_{t-1}^{m'} w_t(T_{t-1}^{m'})}.$$

If the effective sample size $1/\sum_{m=1}^M (W_t^m)^2$ is less than some prespecified threshold (M/10, say), resample the particles.

6. Computing the information of on the current node for its descendants

Given J_t^m, compute $\boldsymbol{\varphi}_i(A_t)$ for $i = 1, \ldots, I$.

3.2 Posterior computation given sampled tree structures

The second stage of our inference strategy is to compute the posterior distributions of the latent states $V(A)$ and the conditional probabilities $\theta_g(A)$ given each sampled tree. We shall focus on the computation of the marginal posterior of the latent states given the tree, as given both the tree and the latent states, the posterior of $\theta_g(A)$ boils down to the corresponding posterior of standard PT models on a one-dimensional space, which is easily evaluable but is problem-specific and is provided in the vast literature on PT models.

The SMC algorithm produces a collection of finite trees $\{T^m\}_{m=1}^M$ along with the importance weights $\{W^m\}_{m=1}^M$. Given each tree T^m, it is possible to analytically calculate the exact posterior of $\{V(A)\}_{A \in T^m}$ with recursive message passing (dynamic programming), which we describe below.

For $A \in \mathcal{N}(T^m)$, let $\phi_A(i)$ be the marginal likelihood on A given the state $V(A) = i$. That is,

$$\phi_A(i) = \int q(\mathbf{x} \mid A) P(dq \mid V(A) = i), \tag{8}$$

where

$$q(\mathbf{x} \mid A) = \prod_{g=1}^{G} \prod_{z \in x_g(A)} q_g(z \mid A).$$

In Eq. (8), taking the integration with respect to $P(dq \mid V(A) = i)$ is equivalent to integrating out $\theta_g(A)$ as well as the $\theta_g(A')$ and $V(A')$ terms for all descendants A' of A. Another useful quantity is the marginal likelihood on a node A given the state of its parent node $V(A^p) = i$, which we denote as $\Phi_A(i)$ and is given by

$$\Phi_A(i) = \begin{cases} \prod_{x \in \mathbf{x}(A)} \mu(x \mid A) & \text{if A is a leaf node,} \\ \sum_{i'=1}^{I} \boldsymbol{\xi}_{i,i'}(A) \phi_A(i') & \text{if A is a non-leaf node.} \end{cases} \tag{9}$$

If $A = \Omega$, only $\Phi_\Omega(1)$ is defined. Note that under this definition, the two quantities are related as

$$\phi_A(i) = M_A(i \mid J(A)) \Phi_{A_l}(i) \Phi_{A_r}(i), \tag{10}$$

where M_A is the marginal likelihood defined in (5) given under the decision $J(A) = (D(A), L(A))$ to divide A into A_l and A_r. By iteratively computing Eqs. (9) and (10) in a bottom-up fashion (i.e., starting from the leafs all the way to the root), we can compute the pair $\{(\phi_A(i), \Phi_A(i)) : A, i\}$ for all nodes in the tree, and this pair is the "message" passed along the tree from leaf to root.

Given the values of $\{(\phi_A(i), \Phi_A(i)) : A, i\}$, we can now obtain the posterior of Markov transition probability matrices of the latent states given the tree

$$\tilde{\boldsymbol{\xi}}(A) = (\tilde{\boldsymbol{\xi}}_{i,i'}(A)) = (P(V(\Omega) = i' \mid V(A^p) = i, \mathbf{x}, T^m))_{i,i'=1}^{I}$$

and the posterior marginal probabilities of the latent states given the tree

$$\tilde{\boldsymbol{\gamma}}(A) = (\tilde{\boldsymbol{\gamma}}_i(A))_{i=1}^{I} = (P(V(\Omega) = i \mid \mathbf{x}, T^m))_{i=1}^{I}.$$

Specifically, by the Bayes' theorem, $\tilde{\boldsymbol{\xi}}(A)$ can be computed as

$$\tilde{\boldsymbol{\xi}}(A) = D_1^{-1}(A)\boldsymbol{\xi}(A)D_2(A),$$

where $D_1(A)$ and $D_2(A)$ are diagonal matrices with $D_1(A)_{i,i} = \Phi_A(i)$ and $D_2(A)_{i,i} = \phi_A(i)$. After we computed these transition matrices, we can compute $\tilde{\boldsymbol{\gamma}}(A)$ (the feedback "message") in the top-down manner (i.e., starting from the root and down to the leafs) based on the following equations:

$$\tilde{\boldsymbol{\gamma}}(\Omega) = \tilde{\boldsymbol{\xi}}_{1,\cdot}(\Omega),\ \tilde{\boldsymbol{\gamma}}(A) = \tilde{\boldsymbol{\gamma}}(A^p)\tilde{\boldsymbol{\xi}}(A) \text{ for } A \neq \Omega. \tag{11}$$

Besides computing the above posterior for the latent states, we note another practical use of the recursive quantity $\Phi_A(i)$. In particular, $\Phi_\Omega(1)$ is the overall marginal likelihood given the tree T^m, $P(\mathbf{x} \mid T^m)$, which can be used to find the *maximum a posteriori* (MAP) tree among the sampled trees, i.e., the one that maximizes $P(T^m \mid \mathbf{x}) \propto P(T^m)P(\mathbf{x} \mid T^m)$. We can use this tree as a point estimate for the tree along with the conditional posterior of the latent states given this tree to visualize and summarize the posterior inference in an interpretable way. For example, as we will demonstrate later in our numerical examples, in two-sample comparison, one can characterize the cross-sample difference by labeling and plotting the nodes in the representative tree along with posterior summaries such as posterior marginal probabilities of the states.

Now that we have completely described our inference algorithm, next we describe two specific examples to demonstrate how one may use the output of the algorithm—namely the sampled trees along with the conditional posterior given the trees—to carry out inference. The first example is density estimation which involves learning the within-sample distributional features while the second is two-sample comparison whose focus is on learning the between-sample structures. The inference strategies for these quintessential examples are generalizable to a variety of other tasks.

Example 1: Density estimation

We consider the problem of estimating a distribution from a single i.i.d. sample, and thus $G = 1$ and so we drop the subscript g to simplify the notation. We shall use the predictive measure—$\mathbb{E}[Q(\cdot) \mid \mathbf{x}]$—as an estimate for Q and the predictive density—$\mathbb{E}[q(\cdot) \mid \mathbf{x}]$—as an estimate for the density $q = dQ/d\mu$.

To this end, we shall first compute for each $A \in T^m$ and $i \in \{1, 2, \ldots, I\}$

$$e_A(i) := \mathbb{E}[Q(A) I_{\{V(A)=i\}} \mid \mathbf{x}]$$

from which we can then obtain

$$\mathbb{E}[Q(B) \mid \mathbf{x}, T^m] = \sum_{A \in \mathcal{L}(T^m)} \frac{\mu(B \cap A)}{\mu(A)} \sum_{i=1}^{I} e_A(i), \;\; B \subset \mathcal{B}(\Omega).$$

The next proposition shows that $e_A(i)$ can be computed by again by top-down message passing.

Proposition 3.2. *For the root node, $e_\Omega(i) = \tilde{\boldsymbol{\gamma}}_{1,i}(\Omega)$. For a non-root node A, $e_A(i)$ can be computed recursively as*

$$e_A(i') = \sum_{i=1}^{I} \tilde{\boldsymbol{\xi}}_{i,i'}(A) \mathbb{E}[\vartheta(A^p) \mid V(A^p) = i, T^m, \mathbf{x}] e_{A^p}(i),$$

where

$$\vartheta(A^p) = \begin{cases} \theta(A^p) & \text{if } A \text{ is the left child of } A^p, \\ 1 - \theta(A^p) & \text{if } A \text{ is the right child of } A^p. \end{cases}$$

The proof is provided in the supplementary materials. After computing $\mathbb{E}[Q(B) \mid \mathbf{x}, T^m]$ for $m = 1, \ldots, M$, we can compute the posterior predictive distribution in the form of a weighted sum

$$\mathbb{E}[Q(B) \mid \mathbf{x}] \approx \sum_{m=1}^{M} W^m \mathbb{E}[Q(B) \mid \mathbf{x}, T^m],$$

along with the posterior predictive density

$$\mathbb{E}[q(x) \mid \mathbf{x}] \approx \sum_{m=1}^{M} W^m \frac{\mathbb{E}[Q(B^m(x)) \mid \mathbf{x}, T^m]}{\mu(B^m(x))},$$

where $B^m(x) \in \mathcal{L}(T^m)$ the leaf node to which x belongs.

Example 2: Two-sample comparison

If we are interested in carrying out the comparison between two (or more) samples using generalizations to the PT models described in Section 2.3.1, we shall compute the posterior probability of the two hypotheses H_0 and H_1. For example, when $V(A)$ are defined as in Eq (4), the posterior probability of the "global" null hypothesis $H_0 : Q_1 = Q_2$ is given by

$$\begin{aligned} P(H_0 \mid \boldsymbol{x}) &= \sum_T P(V(A) \neq 1 \text{ for all } A \in \mathcal{N}(T) \mid T, x) P(T \mid \boldsymbol{x}) \\ &\approx \sum_{m=1}^{M} W^m P(V(A) \neq 1 \text{ for all } A \in \mathcal{N}(T^m) \mid T^m, \mathbf{x}), \end{aligned}$$

where the sum over $\mathcal{T}$ in the first row is over all finite trees with maximum resolution K and the quantity $P(V(A) \in \{2\}$ for all $A \in \mathcal{N}(T^m) \mid T^m, \mathbf{x})$ again is available analytically by message passing (details given in the supplementary materials).

In addition to testing the existence of any difference between samples, in practice it is usually of interest to detect where and how samples differ. To this end, we can report the so-called posterior marginal alternative probability (PMAP) on each node A, along any sampled tree T^m:

$$P(\theta_1(A) \neq \theta_2(A) \mid T^m, \mathbf{x}) = P(V(A) = 1 \mid T^m, \mathbf{x}) = \tilde{\gamma}_i(A).$$

Reporting the PMAPs along a representative tree such as the MAP among the sampled trees can be a particularly useful visualizing tool to help us understand the nature of the underlying difference. Besides reporting the PMAPs, we can also report the estimated extent of the difference using a notion of "effect size" on each A in terms of the log-odds ratio (Soriano and Ma, 2017),

$$\text{eff}(A) = \left| \log\left[\frac{\theta_1(A)}{1-\theta_1(A)}\right] - \log\left[\frac{\theta_2(A)}{1-\theta_2(A)}\right] \right|. \tag{12}$$

which can again be estimated by the posterior expectation $\mathbb{E}[\text{eff}(A) \mid \mathbf{x}]$ using a standard Monte Carlo (not MCMC) sample from the exact posterior given the represenative tree. We will demonstrate this in our later analysis of a mass cytometry data set.

4 Theoretical Properties

Next we investigate the theoretical properties of the proposed model. Previous theoretical analysis on the PT had mostly focused on establishing the marginal posterior consistency and contraction of the random measures Q_g with respect to an underlying truth (Walker

and Hjort, 2001; Castillo, 2017), we shall instead investigate the asymptotic behavior of the marginal posteriors of the partition tree T and the latent states as these are critical quantities of practical importance in data analysis. We note that once given the tree and the latent states, our model reduces to standard PTs and thus the posterior consistency of the random measures Q_g's will follow from previous results once we establish the posterior consistency of the tree and the latent states.

The two key theoretical questions of interest here are:

(1) As the sample size increases, what tree structures, if any, does the marginal posterior of T converges to (i.e., concentrates its mass on)?

(2) How does the posterior of the latent states given the tree behave as sample size grows?

These two questions have broad relevance in inference problems using PT models, and previously several authors have investigated the second question in the two-sample comparison context for their variants of the PT model (Holmes et al., 2015; Soriano and Ma, 2017). In addressing the second question, we aim to provide general results that encompass these previous analyses as special cases. According to our limited knowledge, we are not aware of previous studies on the first question.

We will address each of the two questions in turn. Throughout this section, we consider finite PTs with maximum depth of the trees set to some (potentially large) value K. We use $\mathcal{T}^K$ to denote this collection of trees. Also, while we recommend using a prior for $L(A)$ that depends on the (finite) sample size in practice to achieve good performance in Section 2.2, the asymptotic results are derived under uniform priors on $L(A)$ independent of the sample size. Finally, we consider models that satisfy **Assumption 1** and **Assumption 2** described below. The models discussed in Section 2.3.1 all meet this requirement.

Assumption 1. *The sample size n_g and the true measures P_g for each sample satisfy*

(i) There exists $\zeta_g \in (0,1)$ such that $\zeta_g = \lim_{n\to\infty} \frac{n_g}{n}$ for $g \in 1, \ldots, G$.

(ii) The true sampling distribution P_g satisfies $P_g \ll \mu$, and we let $p_g = dP_g/d\mu$ be the density.

Additionally,

(iii) Given the tree T and the latent states, the parameters $\{\theta_g(A)\}_{g=1}^G$ are given one of the following priors (the model can adopt a mix of these priors for different combinations of A and $V(A)$ values):

Prior A : *$\theta_g(A)$ independently follow a beta prior.*

Prior B : $\theta_1(A) = \cdots = \theta_G(A)$ *and it follows a beta prior.*

Prior C : $\theta_1(A) = \cdots = \theta_G(A) = \mu(A_l)/\mu(A)$.

Establishing the theoretical properties also requires a condition on the latent states. In particular, under some states, the support the prior of the parameters $\{\theta_g(A)\}_{g=1}^G$ needs to include the true values. To describe this requirement, given a tree $T \in \mathcal{T}^K$, let $S_i(A \mid T)$ be the support of the prior of $(\theta_1(A), \ldots, \theta_G(A))$ under the state $V(A) = i$. Then, let $\tau(A \mid T)$ denote the collection of "true states" on A, under which the true probabilities are in the support of the corresponding priors, defined as

$$\tau(A \mid T) = \{i \in \{1, \ldots, I\} : (P_1(A_l \mid A), \ldots, P_G(A_l \mid A)) \in S_i(A \mid T)\}.$$

The next assumption states that the prior for the latent states must give positive probability for all the states to simultaneously take values in $\tau(A \mid T)$.

Assumption 2. *For every* $T \in \mathcal{T}^K$,

$$P(V(A) \in \tau(A \mid T) \text{ for all } A) > 0.$$

With these assumptions, we next derive asymptotic properties for the marginal posteriors for the tree and the state variables. In the following, we use the notation $\mathbf{x}_n$ instead of $\mathbf{x}$ for the data to indicate the total sample size.

4.1 Characterizing the posterior of tree structures

Our first result shows that the marginal likelihood for a node grow at the order of $\exp(n)$.

Proposition 4.1. *For* $T \in \mathcal{T}^K$ *and* $A \in \mathcal{N}(T)$, *define* $N_A(i \mid j_A)$ *as*

$$N_A(i \mid j_A) = M_A(i \mid j_A) \frac{\mu(\mathbf{x}(A_l) \mid A_l)\mu(\mathbf{x}(A_r) \mid A_r)}{\mu(\mathbf{x}(A) \mid A)}.$$

If $i \in \tau(A \mid T)$, *then*

$$\frac{\log N_A(i \mid j_A)}{n} \xrightarrow{p} \sum_{g=1}^{G} \zeta_g P_g(A) \left[P_g(A_l \mid A) \log \frac{P_g(A_l \mid A)}{\mu(A_l \mid A)} + P_g(A_r \mid A) \log \frac{P_g(A_r \mid A)}{\mu(A_r \mid A)} \right]. \quad (13)$$

The function $N_A(i \mid j_A)$ is a main component of h in Eq. (7), and h is interpreted as the likelihood of the decision j_A in the conditional posterior from which we sample in the SMC algorithm. This proposition shows that the speed at which the likelihood grows depends on the way in which a node A is divided. Additionally, the component inside of the square

brackets is the KL divergence between Bernoulli($\mu(A_l \mid A)$) and Bernoulli ($P_g(A_l \mid A)$). Hence, the partition structure that maximizes the weighted sum of the KL divergence will have high probability in the posterior when the sample size is large.

Next we introduce a notion for "tree-based approximation for probability measures". Let T be a finite tree and H a probability measure. Then the "tree-based approximation of H under T", denoted by $H|_T$, is defined as

$$H|_T(B) = \sum_{A \in \mathcal{L}(T)} H(A) \frac{\mu(B \cap A)}{\mu(A)}$$

for any $B \in \mathcal{B}(\Omega)$. The following theorem characterizes the trees that tend to obtain high posterior probability as the sample size grows.

Theorem 4.1. *Let $\mathcal{T}_M^K$ be the collection of trees under which the tree-based approximation of the measures P_g preserves the highest amount of information content as reflected in minimizing the Kullback-Leibler divergence from the P_g's. That is,*

$$\mathcal{T}_M^K = \arg\min_{T \in \mathcal{T}^K} \sum_{g=1}^{G} \zeta_g KL(P_g || P_g|_T). \tag{14}$$

Then the marginal posterior of T concentrates on $\mathcal{T}_M^K$. That is, as $n \to \infty$,

$$P(T \in \mathcal{T}_M^K \mid \mathbf{x}_n) \xrightarrow{p} 1.$$

4.2 Characterizing the posterior of latent states

For the state variables, it is desirable that their posterior distribution concentrate on a collection of "true states". Moreover, when different values of the states capture the truth, it is desirable that their posterior concentrates around values that lead to the most parsimonious representation of the true distributions. (More formal definitions of "true states" and parsimony are given later.) For example, if the true conditional distribution on a node is uniform, a model that introduces a non-uniform structure on this node is redundant. White and Ghosal (2011) and Li and Ghosal (2014) showed that, in quite general settings of multi-resolution inference, the posterior probability of such redundant models tends to converge to 0. By adapting their techniques, we show that the same property holds in the case of our model.

To formally describe the results, we need to define the complexity of the model specified by the latent states. Given the state $V(A) = i$, the complexity of the $\{\theta_g(A)\}_{g=1}^G$, in other words, the number of free parameters of the prior distribution under the ith state is denoted

by $C_i(A)$. For example, for the models for the two-sample problem,

$$C_i(A) = \begin{cases} 2 & \text{if } \theta_1(A) \neq \theta_2(A), \\ 1 & \text{if } \theta_1(A) = \theta_2(A). \end{cases}$$

Next we introduce the complexity of a combination of states on the tree T. Given a tree T, let $\mathbf{V}$ denote a combination of the state variables $\{V(A)\}_{A \in \mathcal{N}(T)}$ and let $\mathbf{v} = \{\mathbf{v}(A)\}_{A \in \mathcal{N}(T)}$ ($\mathbf{v}(A) \in \{1, \ldots, I\}$) be one of the possible realizations of $\mathbf{V}$. Then we define the model complexity under $\mathbf{v}$ as follows:

$$C(\mathbf{v}) = \sum_{A \in \mathcal{N}(T)} C_{\mathbf{v}(A)}(A). \tag{15}$$

The next theorem shows that the posterior distribution of the states given the tree will concentrate on those states that supports the truth while minimizing the complexity at the same time.

Theorem 4.2. *For $T \in \mathcal{T}^K$, let $\mathcal{V}_T = \{\mathbf{v} : \mathbf{v}(A) \in \tau(A \mid T)$ for all $A \in \mathcal{N}(T)\}$. Then we have*

$$P\left(\{\mathbf{V} \in \mathcal{V}_T\} \cap \left\{C(\mathbf{V}) = \min_{\mathbf{v} \in \mathcal{V}_T} C(\mathbf{v})\right\} \mid T, \mathbf{x}_n\right) \xrightarrow{p} 1.$$

From this result, we can derive the consistency provided in the literature as special cases. For example, we derive the consistency for marginal alternative probabilities in the two-sample comparison problem under the MRS model as a corollary from this theorem in the supplementary materials.

5 Experiments

In this section, we carry out simulation studies to examine the performance of our model and inference algorithm. In particular, we are interested in (i) understanding how the model with the flexible tree prior compare to those with a "divide in the middle" restriction, and (ii) verifying the linear scalability of our inference algorithm with respect to increasing dimensionality. We again consider the two quintessential examples—(i) density estimation and (ii) the two-sample problem—for inferring within-sample and between-sample structures. We shall consider both low-dimensional setting where the underlying structure is easy to interpret and software for existing PT models are available, and high-dimensional settings for which existing implementation of PT models is not applicable and we use our SMC algorithm to carry out inference for both our model and the earlier models with fixed partitioning points (which are

special cases of our model). Throughout the experiments, the parameters N_L and M are fixed to 32 and 1000 respectively. We note that larger N_L values can also be adopted at a linear computational cost but did not lead to noticeable change in performance in our examples.

5.1 Density estimation

We first consider 2D examples to observe what kind of tree structures are obtained under the flexible model and how prior specification in Eq. (2) influences the performance. After that, we move to higher dimensional cases to examine the scalability of our new SMC method and the effect of incorporating the flexible partition.

For this task we compare our model with the APT model (Ma, 2017) which also incorporates a prior on the dimension to divide but restrict partitioning at middle points. Following Ma (2017), the transition matrix for the latent states on each A that characterize different smoothness levels of the density is given by

$$\begin{cases} \boldsymbol{\xi}_{i,i'}(A) \propto e^{\beta(i-i')} & \text{if } i \leq i', \\ \boldsymbol{\xi}_{i,i'}(A) = 0 & \text{if } i > i', \end{cases}$$

where $\beta = 0.1$ and the number of states $I = 5$. For the $i(< I)$th state, given $V(A) = i$, the precision $\nu(A)$ follows the prior

$$\log_{10} \nu(A) \sim \text{Unif}(a(i), a(i+1)],$$

where $a(i) = L + (i-1)(U-L)/(I-1)$ with $L = -1$ and $U = 4$. For the Ith state, $F_I = 1_\infty$, so $\nu(A)$ is fixed to ∞. This is equivalent to stopping the partition and putting the conditional distribution $\mu(\cdot \mid A)$ on A. In the computation, this uniform distribution is approximated by 5 evenly spaced grid points.

5.1.1 Two-dimensional cases

Simulated data are generated from the following three scenarios:

1. "Blocks":

$$\frac{1}{3}\mathbf{1}_{[0.1,0.45]\times[0.35,0.9]} + \frac{1}{3}\mathbf{1}_{[0.2,0.8]\times[0.45,0.5]} + \frac{1}{3}\mathbf{1}_{[0.7,0.9]\times[0.05,0.6]}$$

2. "Clusters":

$$\frac{1}{10}Beta(1,1) \times Beta(1,1) + \frac{3}{10}Beta(15,45) \times Beta(15,45) \\ + \frac{3}{10}Beta(45,15) \times Beta(22.5,37.5) + \frac{3}{10}Beta(37.5,22.5) \times Beta(45,15)$$

3. "Smooth":

$$Beta(10, 20) \times Beta(10, 20)$$

The first row in Figure 4 presents the true densities. The first scenario involves boundaries at which the density function is discontinuous while the third scenario has a completely smooth surface. The second scenario is a hybrid of the two in that it contains clusters clear with clear outlines, but the density is smooth within the clusters. We use the our model that equips the APT with flexible partitioning locations under varying strength of the prior on $L(A)$ ($\eta = 0.01$ and 0.1), and compare its performance with the original APT model with the "always dividing in the middle" restriction. For fitting the original APT model, we used the `apt` function in the R package `PTT` (Ma, 2017).

Figure 4 provides a few examples of the estimated density functions and the representative trees. The results for the first scenario confirms that the flexible model is much more effective in capturing the discontinuous boundaries of the true density. For the second scenario, we can see that the flexible model tends to draw the boundaries that surround the true clusters. In the trees given under the different values of η , however, we can see that fewer nodes were divided inside the clusters when $\eta = 0.01$. In contrast, when $\eta = 0.1$, the representative tree draws outlines of the clusters and divides regions inside of the clusters at the same time. A similar phenomenon is observed in the third scenario—under our model with flexible partitioning points, partition lines are formed around the region with high density, when $\eta = 0.1$ for the boundaries were also drawn within the high probability region.

We next quantify the performance of the original APT model and our model in terms of the KL divergence from the true density to the predictive density. Figure 5 provides the average KL divergence based on 300 simulated data sets. The results show that our more flexible model achieves smaller KL divergences only in the first and second scenarios. This phenomenon is related to the fact that in these two scenarios the outlines of regions with high densities are relatively clear, so moving the boundaries toward the outlines tend to improve the accuracy in density estimation. On the other hand, for the third scenario, the tendency of our more flexible model to draw outlines, which does not exist in the smooth surface, incurs a cost on the performance. However, this cost diminishes as n increases, reflected in the fact that the divergence under $\eta = 0.1$ becomes close to the original APT model when the sample size n is large.

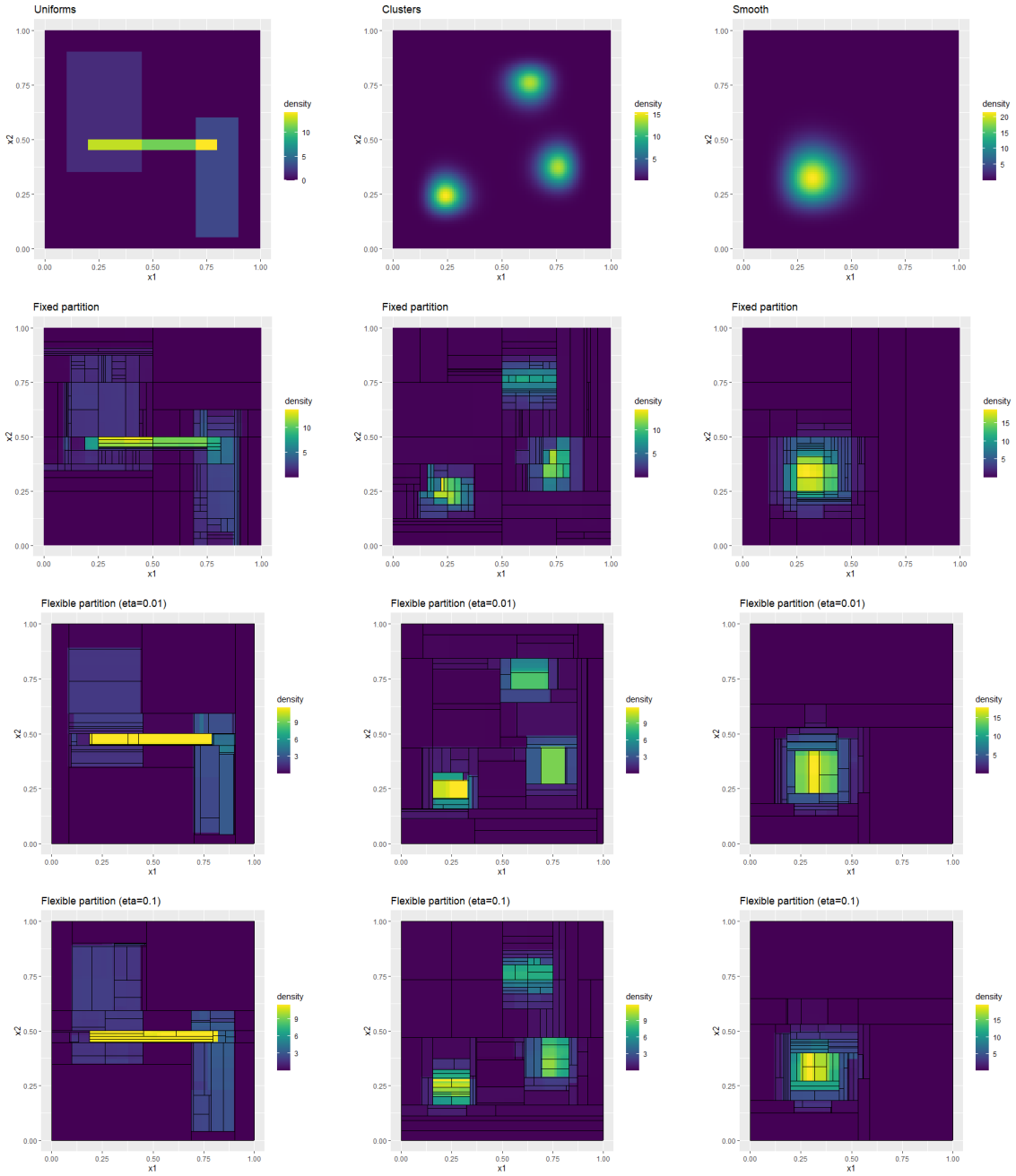

Figure 4: The estimated density functions and the representative trees obtained under $n = 1000$. Each column corresponds to a simulation scenario. The first row shows that true densities, the second row corresponds to the APT model (with fixed partition), and the third and fourth rows correspond to our model with flexible partitioning with parameters $\eta = 0.01$ and 0.1 respectively.

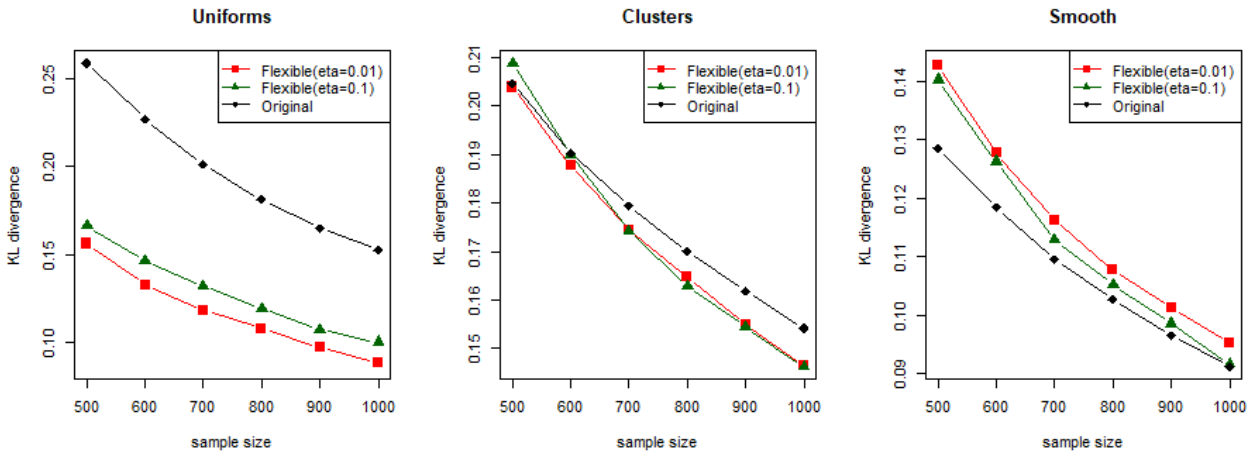

Figure 5: The average KL divergences between the estimated density and the true density.

5.1.2 Higher-dimensional cases

Next we evaluate compare the models under higher dimensional settings. We simulated data sets from the following scenario:

$$\begin{bmatrix} X_1 \\ X_2 \end{bmatrix} \sim \frac{3}{5} Beta(40, 80) \times Beta(40, 80) + \frac{2}{5} Beta(40, 80) \times Beta(90, 30),$$
$$X_3, \ldots, X_d \sim \frac{1}{2} Beta(10, 20) + \frac{1}{2} Beta(20, 10).$$

We consider two different situations: (i) the dimension $d = 5$, and the sample size n changes from 5,000 to 50,000; and (ii) the sample size $n = 10,000$ and the dimensionality changes from 10 to 100. The inference algorithm for the original APT implemented by the `apt` function in the `PTT` package does not scale if the dimension is beyond $d \approx 10$. As such, in the second case with large d, we used the proposed SMC algorithm to carry out inference for the original APT model as well, which corresponds to setting $N_L = 2$. Also, we set the maximum resolution K is fixed to 15.

In Figure 6 we present the computational time for five different data sets. To obtain the result, we used a singe-core environment using Intel Core i5-9400F (2.90 GHz) CPU. The computational time is linear in both the sample size and the dimensionality.

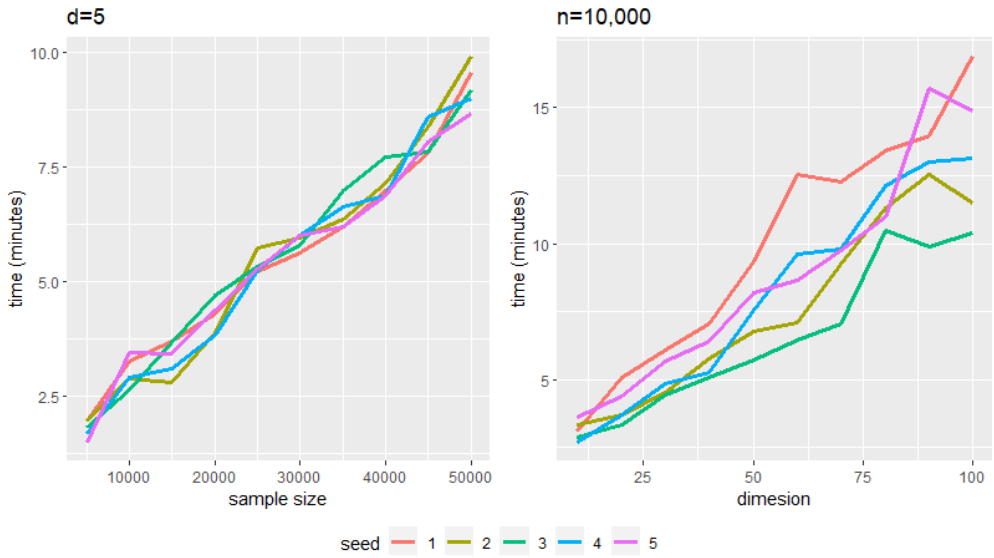

Figure 6: The wall time under five different data sets. The flexible model with $\eta = 0.1$ is used.

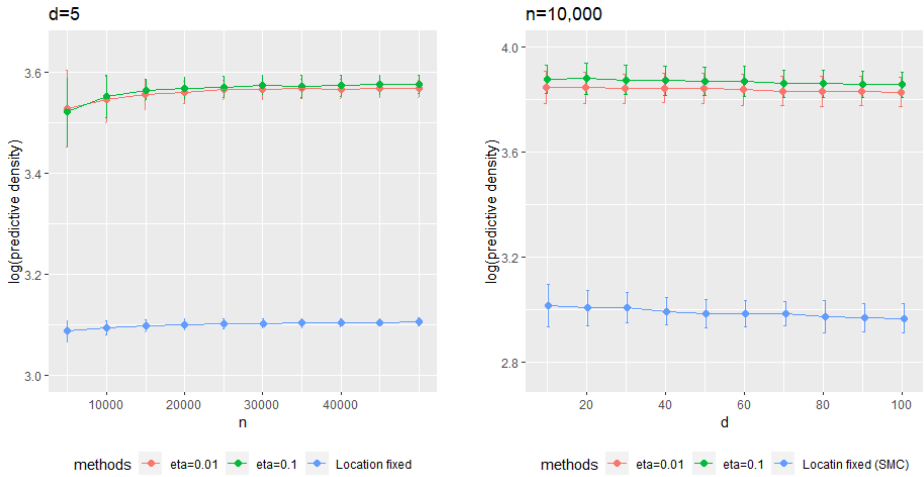

Figure 7: The comparison of the predictive performance. Each point corresponds to the average of the predictive score in Eq. (16) based on 100 data sets. Each interval is formed by adding and subtracting the standard deviation.

Because in the high-dimensional settings we cannot obtain the KL divergence between our estimate and the true density, we compare the models based on predictive scores. Specifically, for the generated data $\mathbf{x}$, we generate a new test set denoted by $\mathbf{x}^* = (x_1^*, \ldots, x_n^*)$ from the

same true model and compute

$$\frac{1}{n}\sum_{i=1}^{n}\log\hat{p}(x_i^* \mid \mathbf{x}), \tag{16}$$

where $\hat{p}$ is the estimated predictive density. We repeat computing the same quantity for 100 different data sets and take their average. The results, given in Figure 7, show that the model with flexible partitioning substantially outperforms the competitor by this criteria both when $d = 5$ with varying sample size and when n is fixed with varying dimensionality.

5.2 Two-sample problem

Next we consider the two-sample comparison problem and evaluate the performance of the MRS model equipped with the flexible partitioning tree prior and compare it to the original MRS with the "always at the moddle" restriction. For the transition matrix $\boldsymbol{\xi}(A)$, we use the form proposed in Soriano and Ma (2017) for achieving multiple testing control

$$\boldsymbol{\xi}(A) = \begin{bmatrix} (1-\rho)\gamma & (1-\rho)(1-\gamma) & \rho \\ (1-\rho)\gamma 2^{-k} & (1-\rho)(1-\gamma 2^{-k}) & \rho \\ 0 & 0 & 1 \end{bmatrix},$$

where $\gamma \in (0,1)$, and $\rho \in (0,1)$, and k is the depth of A. We set $(\gamma, \rho) = (0.3, 0.3)$ as in that paper.

5.2.1 Simulated data

In this experiment, we use the following three scenarios to simulate 50-dimensional data sets. The first two scenarios involve two-sample difference that lie in parts of the sample space, hence are "local" differences, which will help demonstrate how the partition tree can help identify the location and nature of the differences. The sample size is $n_1 = n_2 = 2,000$ in all scenarios.

1. "Local location shift": For $j = 1, \ldots, 25$,

$$(X_{1,2(j-1)+1}, X_{1,2j}) \sim \frac{1}{3}N(\mu_1, \Sigma) + \sum_{l=2}^{3}\frac{1}{3}N(\mu_l, \Sigma),$$

$$(X_{2,2(j-1)+1}, X_{2,2j}) \sim \frac{1}{3}N(\mu_1 + \delta_j, \Sigma) + \sum_{l=2}^{3}\frac{1}{3}N(\mu_l, \Sigma),$$

where $\delta_j = -0.5$ for $j = 1, \ldots, 5$ and 0 for $j = 6, \ldots, 25$.

2. "Local dispersion difference": For $j = 1, \ldots, 25$,

$$(X_{1,2(j-1)+1}, X_{1,2j}) \sim \frac{1}{3}N(\mu_1, \Sigma) + \sum_{l=2}^{3} \frac{1}{3}N(\mu_l, \Sigma),$$
$$(X_{2,2(j-1)+1}, X_{2,2j}) \sim \frac{1}{3}N(\mu_1, \Sigma + \Delta_j) + \sum_{l=2}^{3} \frac{1}{3}N(\mu_l, \Sigma),$$

where $\Delta_j = -0.4$ for $j = 1, \ldots, 5$ and 0 for $j = 6, \ldots, 25$.

3. "Correlation": For $j = 1, \ldots, 25$,

$$(X_{1,2(j-1)+1}, X_{1,2j}) \sim N\left(\begin{bmatrix} 0 \\ 0 \end{bmatrix}, \begin{bmatrix} 1 & 0 \\ 0 & 1 \end{bmatrix}\right)$$
$$(X_{2,2(j-1)+1}, X_{2,2j}) \sim N\left(\begin{bmatrix} 0 \\ 0 \end{bmatrix}, \begin{bmatrix} 1 & \delta_j \\ \delta_j & 1 \end{bmatrix}\right),$$

where $\delta_j = 0.75$ for $j = 1, \ldots, 5$ and $\delta_j = 0$ for $j = 6, \ldots, 25$.

In the "local location shift" and "local dispersion difference", the parameter values are given as

$$\mu_1 = (-2.5, 1.0),\ \mu_2 = (1.0, -2.0),\ \mu_3 = (2.0, 2.5),\ \Sigma = \begin{bmatrix} 0.5 & 0 \\ 0 & 0.7 \end{bmatrix}.$$

The original algorithm for inference under the MRS model by message passing, which is implemented by the `mrs` function in the `R` package `MRS`, is not scalable beyond about 10 dimensions even with fixed partition locations. Hence we compute the posterior for both our model and the original MRS in all scenarios with our SMC and message passing hybrid algorithm. We compare their performance using the receiver operating characteristic (ROC) curves, which are computed based on 200 simulated data sets under each scenario.

Figure 8 presents the ROC curves. For the location shift and dispersion differences, the model with flexible partition locations results in substantially higher sensitivity at each given specificity. On the other hand, for the correlation scenario, the model with fixed partitioning locations performed slightly better. This is not surprising since in this scenario the difference exists smoothly over entire ranges of the dimensions without natural "optimal" division points, and so the performance gap is the cost for searching over more possible partition locations, none of which improves the model fit than the middle point. It is worth noting again that while the model with fixed partitioning performs well here, it is only with our new computational algorithm that it can be fit to data of such dimensionality.

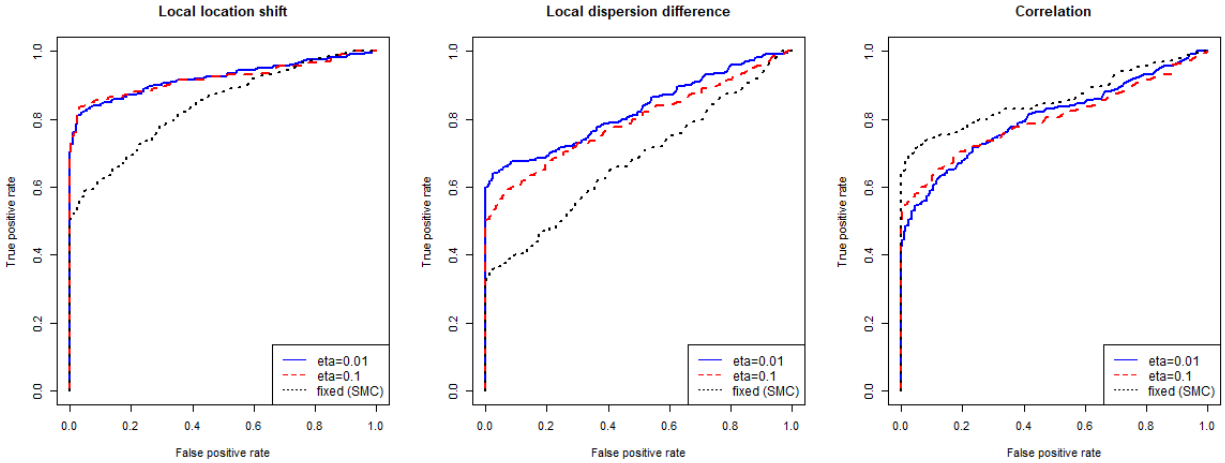

Figure 8: The receiver operating characteristic curves for the 50-dimensional examples.

To demonstrate how one may use the posterior model to understand the nature of the differences, we present under each scenario the node with the highest posterior marginal alternative probability (PMAP), or $P(V(A) = 1 \mid \boldsymbol{x}) = P(\theta_1(A) \neq \theta_2(A) \mid \boldsymbol{x})$, in Figure 9. In the location shift and dispersion difference scenarios the boundaries are away from the middle point to characterize the difference, which partly explains the sensitivity gain in adopting the flexible tree prior.

6 Application to a mass cytometry data set

Finally, we apply the new MRS model with flexible partitioning to a mass cytometry data set collected by Kleinsteuber et al. (2016). The data set records 19 different measurements including physical measurements and biomarkers on single cells in blood samples from a group of HIV patients as well as in reference samples from healthy donors. For demonstration, we compare the sample from an individual patient sample (Patient #1) and to that from a healthy donor to identify differences in immune cell profiles from these samples.

The sample sizes are $29,226$ for the health donor and and $228,498$ for the patient, with each observation corresponding to a cell. We set $\eta = 0.1$ and the maximum resolution K to 25, which is larger than in the previous experiments because we found that the trees need to be deeper to capture all major difference, in the two samples made possible by the large sample sizes.

Given the large sample sizes, the posterior probability for the global alternative $P(Q_1 \neq Q_2 \mid \mathbf{x})$ is almost 1 and so is of less interest. Our focus is instead on identifying the cell subsets

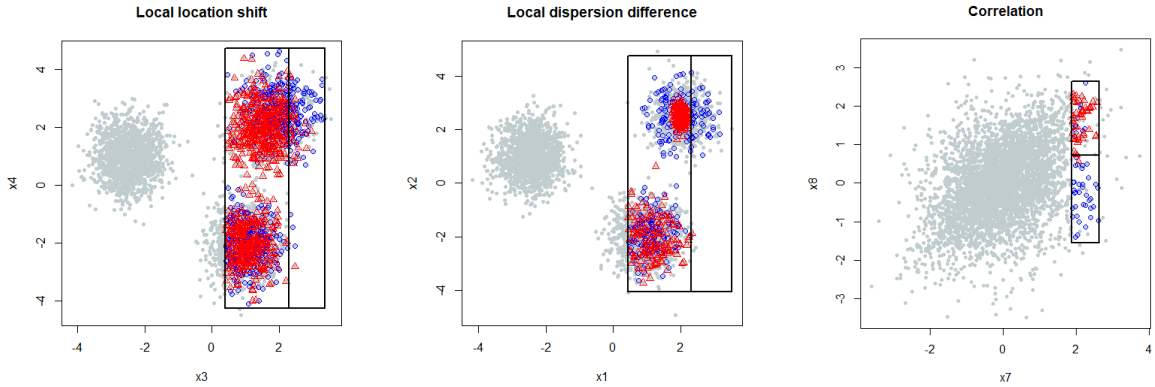

Figure 9: The node with the highest PMAP $P(V(A) = 1 \mid \mathbf{x})$ under the three scenarios for the 50-dimensional example, estimated by the MRS with flexible partitioning and $\eta = 0.1$. The solid lines mark the boundaries of the nodes and the partition line that divides them into the two children nodes. The red triangle points and the blue circle points are the observations of the two groups included in the node. Gray points indicate the observations outside the node.

on which the samples differ and on quantifying such differences. To this end, we identify a representative tree and report the "effect size" (i.e., the posterior expected log-odds ratio between the two samples) on each node in a representative tree—the MAP among the sampled trees—as described in Eq. (12).

The estimated $\text{eff}(A)$'s on the MAP tree is visualized in Figure 10. We note that the nodes on which there is significant evidence for two-sample differences, as well as those with large estimated effect sizes tend to be nested or clustered in subbranches of the tree, which is consistent with our intuition that there is spatial correlation in the two-sample differences, and justifies the hidden Markov structure embedded in the MRS model.

Figure 11 presents the 20 nodes with the largest values of estimated $\text{eff}(A)$. In this figure, many of the nodes are in very deep levels of the tree. We adopted a spike-and-slab with higher spike probability in very deep tree levels to further speed up the computation (details given in supplementary materials) and that explains why many of the very deep, small nodes plotted have partition lines in the middle under the MAP tree.

7 Concluding Remarks

We have proposed a new general framework for the PT model that incorporates a flexible prior on the partition tree and can accommodate latent state variables with Markov structures associated with the partition tree. We have proposed a new inference algorithm that combines

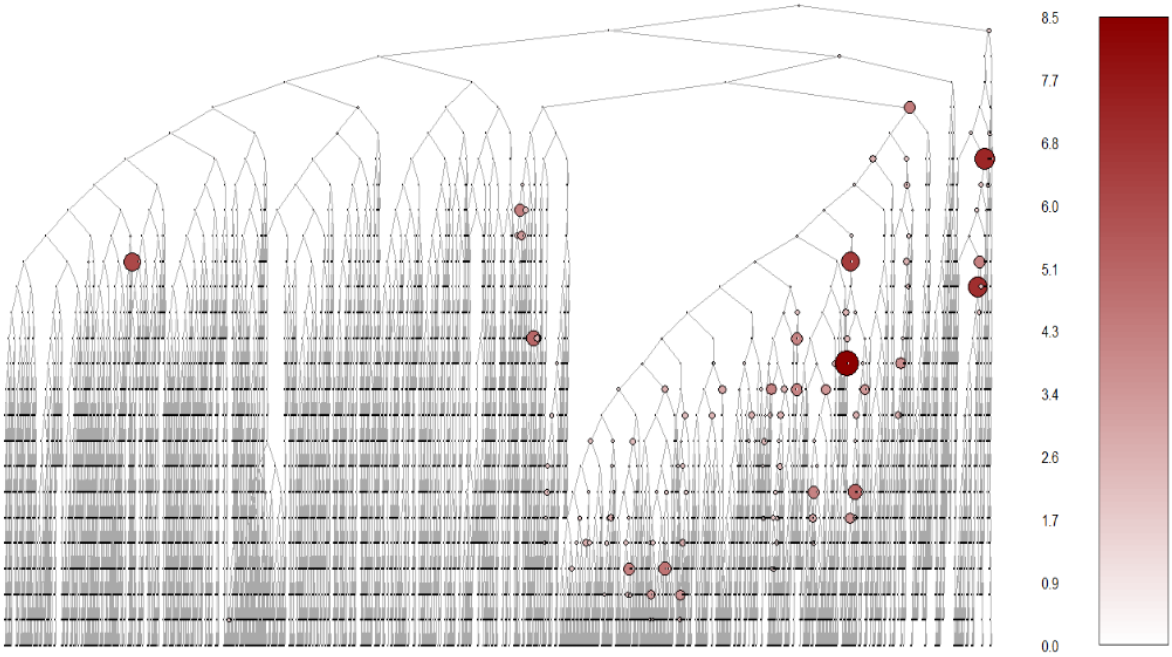

Figure 10: The MAP tree for the mass cytometry data set. The size and the color indicate the estimated $\mathrm{eff}(A)$. Only the nodes with the sample size larger than 50 are drawn.

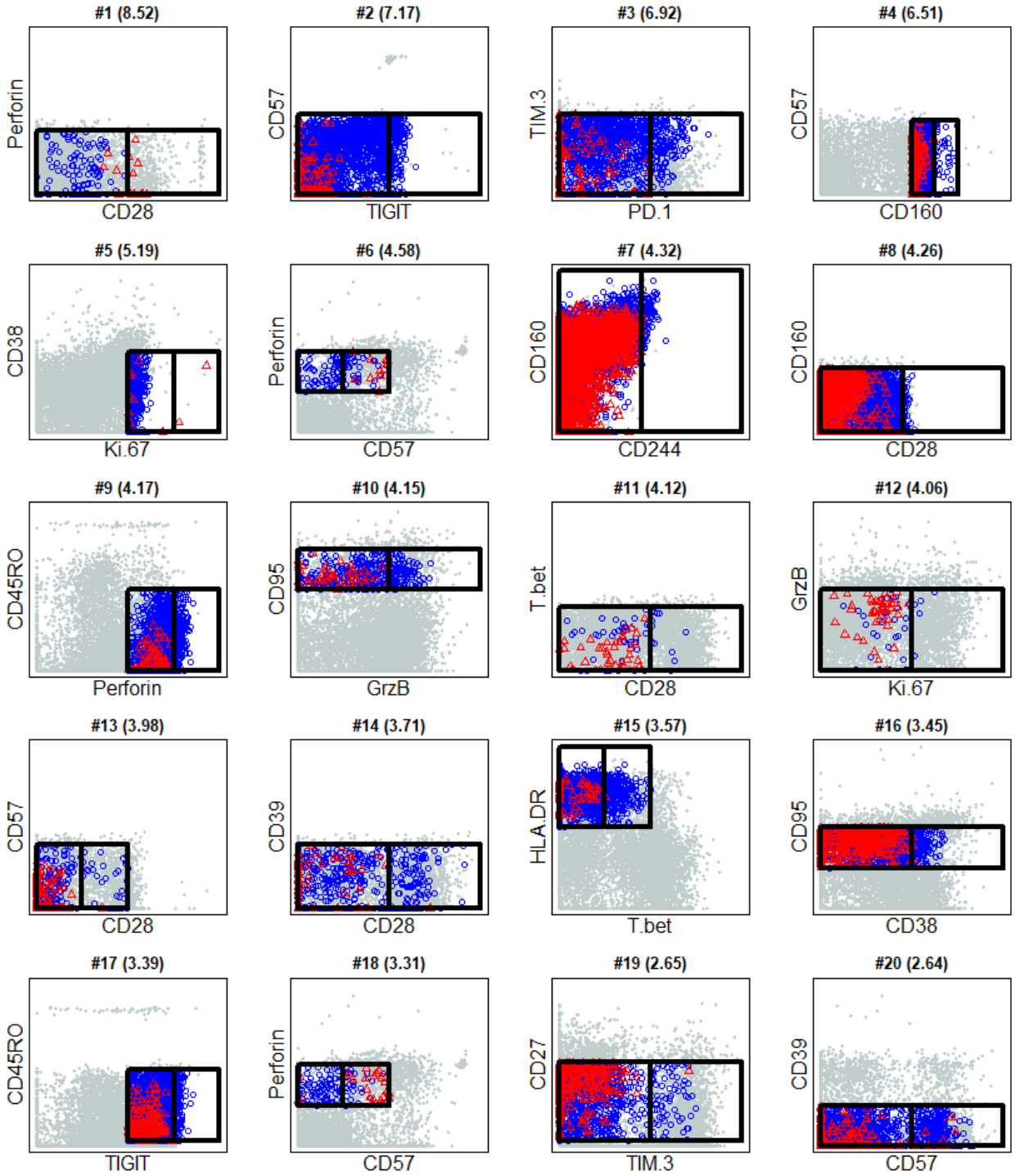

Figure 11: The solid lines delineate the nodes with the highest values of $\mathrm{eff}(A)$ and their two children. The red triangle points and the blue circle points are the observations from the two samples in the node. The observations outside the node are in gray. In this figure, the nodes with $n_g(A) \geq 10$ $(g = 1, 2)$ are chosen.

SMC and recursive message passing to enable the analysis of moderately high-dimensional data. As demonstrated through the numerical experiments, not only is our method computationally efficient in high-dimensional settings, but the flexible partitioning points can results in substantial gain in performance in some settings.

Though we have mainly used two inference tasks—namely density estimation and two-sample comparison—to demonstrate our model and algorithm, our approach can be readily applied to other PT models with a hidden Markov structure.

One notable limitation of our model—and in fact all CART-like models—is that we only consider trees in which the node boundaries are all parallel to the axes. This could lead to inefficiency in inference. For example, when there is a strong correlation between several variables, drawing boundaries slanted according to the correlation structure would be more effective in characterizing the underlying distribution. Such tree structures will need to be represented by more than just the $D(A)$ and $L(A)$ used in our model, and how to efficiently compute their posterior distributions is of interest in future studies.

Acknowledgment

LM's research is partly supported by NSF grants DMS-2013930 and DMS-1749789. NA is partly supported by a fellowship from the Nakajima Foundation.

References

James O Berger and Alessandra Guglielmi. Bayesian and conditional frequentist testing of a parametric model versus nonparametric alternatives. *Journal of the American Statistical Association*, 96(453):174–184, 2001.

Ismaël Castillo. Pólya tree posterior distributions on densities. In *Annales de l'Institut Henri Poincaré, Probabilités et Statistiques*, volume 53, pages 2074–2102. Institut Henri Poincaré, 2017.

Yuhui Chen and Timothy E Hanson. Bayesian nonparametric k-sample tests for censored and uncensored data. *Computational Statistics & Data Analysis*, 71:335–346, 2014.

Jonathan Christensen. *Applications and Computation of Stateful Polya Trees*. PhD thesis, Duke University, 2017.

Jonathan Christensen and Li Ma. A bayesian hierarchical model for related densities by using pólya trees. *Journal of the Royal Statistical Society: Series B (Statistical Methodology)*, 2019.

Matthew S Crouse and Richard G Baraniuk. Contextual hidden markov models for wavelet-domain signal processing. In *Conference Record of the Thirty-First Asilomar Conference on Signals, Systems and Computers (Cat. No. 97CB36136)*, volume 1, pages 95–100. IEEE, 1997.

Thomas S Ferguson. A bayesian analysis of some nonparametric problems. *The annals of statistics*, pages 209–230, 1973.

Thomas S Ferguson. Prior distributions on spaces of probability measures. *The annals of statistics*, 2(4):615–629, 1974.

Sarah Filippi, Chris C Holmes, et al. A bayesian nonparametric approach to testing for dependence between random variables. *Bayesian Analysis*, 12(4):919–938, 2017.

David A Freedman. On the asymptotic behavior of bayes' estimates in the discrete case. *The Annals of Mathematical Statistics*, pages 1386–1403, 1963.

Timothy Hanson and Wesley O Johnson. Modeling regression error with a mixture of polya trees. *Journal of the American Statistical Association*, 97(460):1020–1033, 2002.

Timothy E Hanson. Inference for mixtures of finite polya tree models. *Journal of the American Statistical Association*, 101(476):1548–1565, 2006.

Chris C Holmes, François Caron, Jim E Griffin, David A Stephens, et al. Two-sample bayesian nonparametric hypothesis testing. *Bayesian Analysis*, 10(2):297–320, 2015.

Alejandro Jara and Timothy E Hanson. A class of mixtures of dependent tail-free processes. *Biometrika*, 98(3):553–566, 2011.

Katja Kleinsteuber, Björn Corleis, Narges Rashidi, Nzuekoh Nchinda, Antonella Lisanti, Josalyn L Cho, Benjamin D Medoff, Douglas Kwon, and Bruce D Walker. Standardization and quality control for high-dimensional mass cytometry studies of human samples. *Cytometry Part A*, 89(10):903–913, 2016.

Balaji Lakshminarayanan, Daniel Roy, and Yee Whye Teh. Top-down particle filtering for bayesian decision trees. In *International Conference on Machine Learning*, pages 280–288, 2013.

Michael Lavine et al. Some aspects of polya tree distributions for statistical modelling. *The annals of statistics*, 20(3):1222–1235, 1992.

Meng Li and Subhashis Ghosal. Bayesian multiscale smoothing of gaussian noised images. *Bayesian analysis*, 9(3):733–758, 2014.

Luo Lu, Hui Jiang, and Wing H Wong. Multivariate density estimation by bayesian sequential partitioning. *Journal of the American Statistical Association*, 108(504):1402–1410, 2013.

Li Ma. Adaptive testing of conditional association through recursive mixture modeling. *Journal of the American Statistical Association*, 108(504):1493–1505, 2013.

Li Ma. Adaptive shrinkage in pólya tree type models. *Bayesian Analysis*, 12(3):779–805, 2017.

Li Ma and Jacopo Soriano. Analysis of distributional variation through multi-scale beta-binomial modeling. *arXiv preprint arXiv:1604.01443*, 2016.

Li Ma and Jacopo Soriano. Efficient functional anova through wavelet-domain markov groves. *Journal of the American Statistical Association*, 113(522):802–818, 2018.

Li Ma and Wing Hung Wong. Coupling optional pólya trees and the two sample problem. *Journal of the American Statistical Association*, 106(496):1553–1565, 2011.

Pietro Muliere and Stephen Walker. A bayesian non-parametric approach to survival analysis using polya trees. *Scandinavian Journal of Statistics*, 24(3):331–340, 1997.

Andrew A Neath. Polya tree distributions for statistical modeling of censored data. *Advances in Decision Sciences*, 7(3):175–186, 2003.

Luis E Nieto-Barajas and Peter Mueller. Rubbery polya tree. *Scandinavian Journal of Statistics*, 39(1):166–184, 2012.

Susan M Paddock. Bayesian nonparametric multiple imputation of partially observed data with ignorable nonresponse. *Biometrika*, 89(3):529–538, 2002.

Susan M Paddock, Fabrizio Ruggeri, Michael Lavine, and Mike West. Randomized polya tree models for nonparametric bayesian inference. *Statistica Sinica*, pages 443–460, 2003.

Gideon Schwarz et al. Estimating the dimension of a model. *The annals of statistics*, 6(2): 461–464, 1978.

Jacopo Soriano and Li Ma. Probabilistic multi-resolution scanning for two-sample differences. *Journal of the Royal Statistical Society: Series B (Statistical Methodology)*, 79(2):547–572, 2017.

Stephen Walker and Nils Lid Hjort. On bayesian consistency. *Journal of the Royal Statistical Society: Series B (Statistical Methodology)*, 63(4):811–821, 2001.

Stephen G Walker and Bani K Mallick. Hierarchical generalized linear models and frailty models with bayesian nonparametric mixing. *Journal of the Royal Statistical Society: Series B (Statistical Methodology)*, 59(4):845–860, 1997.

Stephen G Walker, Paul Damien, Purushottam W Laud, and Adrian FM Smith. Bayesian nonparametric inference for random distributions and related functions. *Journal of the Royal Statistical Society: Series B (Statistical Methodology)*, 61(3):485–527, 1999.

John Thomas White and Subhashis Ghosal. Bayesian smoothing of photon-limited images with applications in astronomy. *Journal of the Royal Statistical Society: Series B (Statistical Methodology)*, 73(4):579–599, 2011.

Samuel S Wilks. The large-sample distribution of the likelihood ratio for testing composite hypotheses. *The Annals of Mathematical Statistics*, 9(1):60–62, 1938.

Wing H Wong and Li Ma. Optional pólya tree and bayesian inference. *The Annals of Statistics*, 38(3):1433–1459, 2010.

A Spike-and-slab type prior for $L(A)$

A.1 Introducing an auxiliary variable

The location variable $L(A)$ follows a spike-and-slab type prior which is expressed with an auxiliary variable $R(A)$ as

$$L(A) \mid R(A) \sim \mathbf{1}_{\{R(A)=1\}}\delta_{1/2}(\cdot) + \mathbf{1}_{\{R(A)=0\}} \sum_{l=1, l/N_L \neq 1/2}^{N_L-1} \hat{\beta}_l(A)\delta_{l/N_L}(\cdot),$$

where $\mathbf{1}$ is the indicator function and the sum of the parameters $\beta_l(A)$ is 1. Under this prior, $L(A)$ follows the prior degenerated at $1/2$ if $R(A) = 1$ and otherwise follows the distribution on grid points other than the middle point. $R(A)$ follows an asymmetric hidden Markov process

$$P(R(A) = 1 \mid R(A^p) = 0) = r(A),$$
$$P(R(A) = 1 \mid R(A^p) = 1) = 1,$$

where $r(A) \in [0, 1]$. $R(A) = 1$ is the absorbing state, so once A is divided at the middle point, $L(A') = 1/2$ for every A's descendant node A'. In the estimation we especially set the parameters as follows:

$$r(A) = \beta_{N_L/2},\ \hat{\beta}_l = \frac{\beta_l(A)}{\sum_{l=1, l/N_L \neq 1/2}^{N_L-1} \beta_l(A)},$$

where $\beta_l(A)$ is given in (2). Under this setting the prior of $L(A)$ satisfies

$$P(L(A) = l \mid R(A^p) = 0) = \beta_l(A),\ l = 1, \ldots, N_L - 1.$$

Hence, $L(A)$ follows the same prior as defined in (1) unless A's parent node is divided at the middle point, so the spike-and-slab prior can be seen as a natural extension.

A.2 SMC algorithm

In the SMC algorithm, we sample values of $R(A)$ in addition to $D(A)$ and $L(A)$. If $R(A) = 1$, which is equivalent to $L(A) = 1/2$, is sampled, we conclude there is no interesting structure on the node A so fix L to $1/2$ for all the subsequent nodes. Hence, we need to generalize the SMC algorithm discussed in Section 3.1 to sample from the joint posterior distribution of the finite trees and the auxiliary variables R.

To describe this joint posterior, let T_t denote the finite tree structure, which is determined by the sequence of decisions $J_{1:t}$ dividing the nodes $A_{1:t}$, and let $R_{1:t}$ be a sequence of the

re-fixing variables for $A_{1:t}$. Then the target distribution we want to sample from in the SMC is defined as

$$\pi_t(T_t, R_{1:t}) = P(T_t, R_{1:t} \mid \mathbf{x}) \propto P(T_t, R_{1:t}) P(\mathbf{x} \mid T_t, R_{1:t}).$$

The prior $P(T_t, R_{1:t}) = P(J_{1:t}, R_{1:t})$ have a Markov chain structure on the tree, and its transition probability is decomposed as

$$P(J_t, R_t \mid J_t^p, R_t^p) = P(R_t \mid R_t^p) P(J_t).$$

where $J_t^p = J(A_t^p)$ and $R_t^p = R(A_t^p)$ (A_t^p is the parent node of A_t). On the other hand, because $R_{1:t}$ are conditionally independent of the observations given T_t, the likelihood only depends on T_t as follows:

$$P(\mathbf{x} \mid T_t, R_{1:t}) = P(\mathbf{x} \mid T_t).$$

The likelihood has the same form as in the original case without the auxiliary variables R's. Thus we can obtain the following proposition as a generalization of Proposition 3.1.

Proposition A.1. *Let $h(J_t \mid A_t)$ be a function of J_t defined as*

$$h(J_t \mid A_t) = \sum_{i=1}^{I} \left\{ \sum_{j=1}^{I} \boldsymbol{\varphi}_j(A_t^p) \boldsymbol{\xi}_{j,i}(A_t) \right\} M_i(A_t \mid J_t) \frac{\mu(\mathbf{x}(A_{t,l}) \mid A_{t,l}) \mu(\mathbf{x}(A_{t,r}) \mid A_{t,r})}{\mu(\mathbf{x}(A_t) \mid A_t)}.$$

Then the target distribution $\pi_t(T_t, R_{1:t})$ is expressed with $\pi_t(T_{t-1}, R_{1:t-1})$ as

$$\pi_t(T_t, R_t) = C \pi_t(T_{t-1}, R_{1:t}) \pi_t(R_t \mid T_{t-1}, R_t^p) \pi_t(J_t \mid T_{t-1}, R_t) w_t(T_{t-1}, R_t^p),$$

where C is a constant and

$$\pi_t(R_t \mid T_{t-1}, R_t^p) = \frac{P(R_t \mid R_t^p) \sum_{j_t} P(j_t \mid R_t) h(j_t \mid A_t)}{\sum_{i=0,1} P(R_t = i \mid R_t^p) \left\{ \sum_{j_t} P(j_t \mid R_t = i) h(j_t \mid A_t) \right\}},$$

$$\pi_t(J_t \mid T_{t-1}, R_t) = \frac{P(J_t \mid R_t) h(J_t \mid A_t)}{\sum_{j_t} P(j_t \mid R_t) h(j_t \mid A_t)},$$

$$w_t(T_{t-1}, R_t^p) = \sum_{i=0,1} P(R_t = i \mid R_t^p) \left\{ \sum_{j_t} P(j_t \mid R_t = i) h(j_t \mid A_t) \right\}.$$

The summation with j_t is taken over all possible decisions.

Its proof is essentially the same as Proposition 3.1 so it is omitted in this material. The conditional posteriors $\pi_t(R_t \mid R_t^p, T_{t-1})$ and $\pi_t(J_t \mid R_t, T_{t-1})$ are analytically obtained as follows.

First, if $R_t^p = 0$, $\pi_t(R_t \mid R_t^p, T_{t-1})$ is $Bernoulli(\tilde{r}(A_t))$, where

$$\tilde{r}(A_t) = r(A_t) \sum_{j=1}^{J} \lambda_j(A_t) h((j, 1/2) \mid A_t)$$
$$\times \left[r(A_t) \sum_{j=1}^{J} \lambda_j(A_t) h((j, 1/2) \mid A_t) + (1 - r(A_t)) \sum_{j=1}^{J} \sum_{l=1}^{N_L - 1} \lambda_j(A_t) \beta_l(A_t) h((j, l/N_L) \mid A_t) \right]^{-1},$$

If $R_t^p = 1$, then R_t is fixed to 1. Second, if $R_t = 0$, the posterior of D_t and L_t is the same distribution given in Section 3.1. On the other hand, if $R_t = 1$, L_t is fixed to 1/2, and the conditional posterior $\pi_t(J_t \mid L_t, R_t, T_{t-1})$ is $Multi(\hat{\lambda}_1(A_t), \ldots, \hat{\lambda}_d(A_t))$, where

$$\hat{\lambda}_j(A_t) \propto \lambda_j(A_t) h(j, 1/2 \mid A_t).$$

After sampling (R_t, J_t), the incremental weight $w_t(T_{t-1}, R_t^p)$ $(R_t^p = 0, 1)$ is computed as

$$w_t(T_{t-1}, 0)$$
$$= r(A_t) \sum_{j=1}^{J} \lambda_j(A_t) h((j, 1/2) \mid A_t) + (1 - r(A_t)) \sum_{j=1}^{J} \sum_{l=1}^{N_L - 1} \lambda_j(A_t) \beta_l(A_t) h((j, l/N_L) \mid A_t),$$
$$w_t(T_{t-1}, 1) = \sum_{j=1}^{J} \lambda_j(A_t) h((j, 1/2) \mid A_t),$$

with which we update the importance weight W_t as $W_t \propto W_{t-1} w_t(T_{t-1}, R_t^p)$.

The procedure to update the particle system $\{T_{t-1}^m, W_{t-1}^m\}_{m=1}^M$ to obtain $\{T_t^m, W_t^m\}_{m=1}^M$ is described in the following algorithm. The operations involving the index m is repeated for $m = 1, \ldots, M$.

---

1. Choosing the current node

From T_{t-1}^m, choose the oldest note from the leaf nodes, which is denoted by A_t.

2. Obtaining the information of the parent node

Pick up A_t's parent node, which is denoted by A_t^p, and load the values of $\boldsymbol{\varphi}_i(A_t^p)$ for $i = 1, \ldots, I$ and $R_t^{m,p} = R(A_t^p)$.

3. Computing the necessary quantities

If $R_t^{m,p} = 0$, compute $M_i(A \mid j, l/N_L)$ $(i = 1, \ldots, I)$ and $h(j, l/N_L \mid A_t)$ for $j = 1, \ldots, d$ and $l = 1, \ldots, N_L - 1$.

If $R_t^{m,p} = 1$, compute $M_i(A \mid j, 1/2)$ $(i = 1, \ldots, I)$ and $h(j, 1/2 \mid A_t)$ for $j = 1, \ldots, d$.

4. Deciding whether to fix the partition or not

If $R_t^{m,p} = 0$, compute the parameter $\tilde{r}(A_t)$ and draw $R_t^m \sim Bernoulli(\tilde{r}(A_t))$.
If $R_t^{m,p} = 1$, set R_t^m to be 1.

5. Dividing the current node

Sample $J_t^m = (D_t^m, L_t^m)$ as follows:

- If $R_t^m = 0$, compute the parameters $\tilde{\lambda}_j(A_t)$ for $j = 1, \ldots, d$ and sample

$$D_t^m \sim Multi(\tilde{\lambda}_1(A_t), \ldots, \tilde{\lambda}_d(A_t)).$$

  Given D_t^m, compute the parameters $\tilde{\beta}_l(A_t)$ for $l = 1, \ldots, N_L - 1$ and sample

$$L_t^m \sim \sum_{l=1}^{N_L-1} \tilde{\beta}_l(A_t)\delta_{l/N_L}(\cdot).$$

- If $R_t^m = 1$, compute the parameters $\hat{\lambda}_j(A_t)$ for $j = 1, \ldots, d$ and sample

$$D_t^m \sim Multi(\hat{\lambda}_1(A_t), \ldots, \hat{\lambda}_d(A_t)),$$

  and set $L_t^m = 1/2$.

Divide the current node A_t with $J_t^m = (D_t^m, L_t^m)$ to obtain the updated tree T_t^m.

6. Storing the information of the state's posterior

Given J_t^m, compute $\boldsymbol{\varphi}_i(A_t)$ for $i = 1, \ldots, I$ and store them to the memory.

7. Updating the importance weight

Compute the incremental weight $w_t(T_{t-1}^m, R_t^{m,p})$ and update the importance weights as

$$W_t^m = \frac{W_{t-1}^m w_t(T_{t-1}^m, R_t^{m,p})}{\sum_{m'=1}^M W_{t-1}^{m'} w_t(T_{t-1}^{m'}, R_t^{m',p})}.$$

If the effective sample size $1/\sum_{m=1}^M (W_t^m)^2$ is less than some prespecified threshold (M/10, say), resample the particles.

B Additional algorithm for the MRS model

To describe the algorithm proposed in Soriano and Ma (2017), we keep using the same notations in 3.2. Given the tree structure T, we compute functions $\tilde{\psi}(A)$ for $A \in \mathcal{N}(T)$ in the bottom-up (from the leaf nodes to the root node) manner as follows:

$$\tilde{\psi}(A) = \begin{cases} \tilde{\boldsymbol{\xi}}_{2,2}(A) + \tilde{\boldsymbol{\xi}}_{2,3}(A) & \text{if } A \in \mathcal{L}(T), \\ \tilde{\boldsymbol{\xi}}_{2,2}(A)\tilde{\psi}(A_l)\tilde{\psi}(A_r) + \tilde{\boldsymbol{\xi}}_{2,3}(A) & \text{if } A \in \mathcal{N}(T) \setminus \{\Omega\}, \\ \tilde{\boldsymbol{\xi}}_{1,2}(A)\tilde{\psi}(A_l)\tilde{\psi}(A_r) + \tilde{\boldsymbol{\xi}}_{1,3}(A) & \text{if } A = \Omega. \end{cases}$$

Recall that only the first row of $\boldsymbol{\xi}(\Omega)$ is meaningful as the initial distribution. Then we obtain $\tilde{\psi}(\Omega) = P(H_0 \mid T, \mathbf{x})$.

C Proofs

Proof of Proposition 3.1

Let the finite tree T_t consist of a sequence of decisions $J_{1:t} = \{J_s\}_{s=1}^t$, which sequentially devides nodes $A_{1:t} = \{A_s\}_{s=1}^t$. To derive the proposition for the marginal posterior of T_t, we first consider the joint posterior of T_t and a sequence of the state variables $V_{1:t}$ which are defined for the nodes $A_{1:t}$. From the structure of the model, the joint posterior is written as

$$\begin{aligned} \pi_t(T_t, V_{1:t}) &= P(J_{1:t}, V_{1:t} \mid \mathbf{x}) \\ &= \frac{1}{Z_t} P(J_{1:t}) P(V_{1:t}) \prod_{s=1, A_s \in \mathcal{N}(T_t)}^{t} M_{V_s}(A_s \mid J_s) \prod_{s=1, A_s \in \mathcal{L}(T_t)}^{t} \mu(\mathbf{x}(A_s) \mid A_s), \end{aligned} \tag{17}$$

where Z_t is the normalizing constant, and $A_{s,l}$ and $A_{s,r}$ are the children nodes of A_s. For this posterior, we use the following lemma to prove Proposition 3.1.

Lemma C.1. *For the finite tree T_t, let A_s be a node whose children nodes are leaf nodes. Then we have*

$$\pi_t(V_s = i \mid T_t) = \frac{\pi_t(T_t, V_s = i)}{\pi_t(T_t)} = \boldsymbol{\varphi}_i(A_s),$$

where $\boldsymbol{\varphi}_i(A_s)$ is defined in (6).

(Proof) Suppose that A_s belongs to the kth layer of T_t. Then there is a sub-sequence $\{\rho(l)\}_{l=1}^k$ such that $A_{\rho(l)}$ belongs to the lth layer and

$$\Omega = A_{\rho(1)} \supset A_{\rho(2)} \supset \cdots \supset A_{\rho(k)} = A_s.$$

By the definition of $\pi_t(T_t, V_{1:t})$, for a sequence $\{v_l\}_{l=1}^k$ such that $v_l \in \{1, \ldots, I\}$, we obtain the expression of the conditional posterior of $\{V_{\rho(l)}\}_{l=1}^k$ as

$$\begin{aligned}\pi_t(\{V_{\rho(l)}\}_{l=1}^k = \{v_l\}_{l=1}^k \mid T_t) &\propto P(\{V_{\rho(l)}\}_{l=1}^k = \{v_l\}_{l=1}^k) \prod_{l=1}^k M_{v_l}(A_{\rho(l)} \mid J_{\rho(l)}) \\ &= \prod_{l=1}^k \boldsymbol{\xi}_{v_{l-1},v_l}(A_{\rho(l)}) M_{v_l}(A_{\rho(l)} \mid J_{\rho(l)}),\end{aligned}$$

where $v_0 = 1$. We show that for every $k = 1, \ldots, K$

$$\begin{aligned}\pi_t(V_{\rho(k)} = v_k \mid T_t) &\propto \sum_{v_1=1}^I \cdots \sum_{v_{k-1}=1}^I \left\{ \prod_{l=1}^k \boldsymbol{\xi}_{v_{l-1},v_l}(A_{\rho(l)}) M_{v_l}(A_{\rho(l)} \mid J_{\rho(l)}) \right\} \\ &\propto \boldsymbol{\varphi}_{v_k}(A_s) \end{aligned} \tag{18}$$

holds by induction. First, if $k = 1$, which is equivalent to $s = 1$, $\rho(1) = 1$, and $A_s = \Omega$, the posterior of $V(\Omega)$ is written as

$$\pi_t(V(\Omega) = v_1 \mid T_t) \propto \boldsymbol{\xi}_{1,v_1}(\Omega) M_{v_1}(A_1 \mid J_1) \propto \boldsymbol{\varphi}_{v_1}(\Omega).$$

Second, assume that (18) holds for $k = \bar{k}$. Then, if $k = \bar{k} + 1$, we have

$$\begin{aligned}&\pi_t(V_{\bar{k}} = v_{\bar{k}}, V_{\bar{k}+1} = v_{\bar{k}+1} \mid T_t) \\ &\propto \sum_{v_1=1}^I \cdots \sum_{v_{\bar{k}-1}=1}^I \pi_t(\{V_{\rho(l)}\}_{l=1}^{\bar{k}+1} = \{v_l\}_{l=1}^{\bar{k}+1} \mid T_t) \\ &\propto \sum_{v_1=1}^I \cdots \sum_{v_{\bar{k}-1}=1}^I \left\{ \prod_{l=1}^{\bar{k}} \boldsymbol{\xi}_{v_{l-1},v_l}(A_{\rho(l)}) M_{v_l}(A_{\rho(l)} \mid J_{\rho(l)}) \right\} \boldsymbol{\xi}_{v_{\bar{k}},v_{\bar{k}+1}}(A_s) M_{v_{\bar{k}+1}}(A_s \mid J_s) \\ &\propto \boldsymbol{\varphi}_{v_{\bar{k}}}(A_{\rho(\bar{k})}) \boldsymbol{\xi}_{v_{\bar{k}},v_{\bar{k}+1}}(A_s) M_{v_{\bar{k}+1}}(A_s \mid J_s),\end{aligned}$$

from which we obtain

$$\begin{aligned}\pi_t(V_{\bar{k}+1} = v_{\bar{k}+1} \mid T_t) &= \sum_{v_{\bar{k}}=1}^I \pi_t(V_{\bar{k}} = v_{\bar{k}}, V_{\bar{k}+1} = v_{\bar{k}+1} \mid T_t) \\ &\propto \sum_{v_{\bar{k}}=1}^I \boldsymbol{\varphi}_{v_{\bar{k}}}(A_{\rho(\bar{k})}) \boldsymbol{\xi}_{v_{\bar{k}},v_{\bar{k}+1}}(A_s) M_{v_{\bar{k}+1}}(A_s \mid J_s) \\ &\propto \boldsymbol{\varphi}_{v_{\bar{k}+1}}(A_s). \quad \square\end{aligned}$$

(Proof of Proposition 3.1)
For T_{t-1} and T_t, since A_t is divided into $A_{t,l}$ and $A_{t,r}$, we have

$$\mathcal{N}(T_t) = \mathcal{N}(T_{t-1}) \cup \{A_t\},$$
$$\mathcal{L}(T_t) = \mathcal{L}(T_{t-1}) \setminus \{A_t\} \cup \{A_{t,l}, A_{t,r}\}.$$

With the expression of the joint posterior in (17), we obtain

$$\pi_t(T_t, V_{1:t}) = \frac{Z_t}{Z_{t-1}} \pi_{t-1}(T_{t-1}, V_{1:t-1}) P(J_t) P(V_t \mid V_{1:t-1}) M_{V_t}(A_t \mid J_t) \frac{\mu(\mathbf{x}(A_{s,l}) \mid A_{t,l}) \mu(\mathbf{x}(A_{s,r}) \mid A_{s,r})}{\mu(\mathbf{x}(A_s) \mid A_s)}. \tag{19}$$

Let A_t^p denote the parent node of A_t and $V_t^p = V(A_t^p)$. Then, since the state variables follow the hidden Markov process, $P(V_t \mid V_{1:t-1}) = \boldsymbol{\xi}_{V_t^p, V_t}(A_t)$. Integrating out $V_{1:t-1} \setminus V_t^p$ in (19) gives

$$\pi_t(T_t, V_t^p, V_t) = \frac{Z_t}{Z_{t-1}} \pi_{t-1}(T_{t-1}, V_t^p) P(J_t) \boldsymbol{\xi}_{V_t^p, V_t}(A_t) M_{V_t}(A_t \mid J_t) \frac{\mu(\mathbf{x}(A_{s,l}) \mid A_{t,l}) \mu(\mathbf{x}(A_{s,r}) \mid A_{s,r})}{\mu(\mathbf{x}(A_s) \mid A_s)}.$$

Because A_t is a leaf node of T_{t-1}, by Lemma C.1, we have

$$\begin{aligned}\pi_{t-1}(T_{t-1}, V_t^p = j) &= \pi_{t-1}(T_{t-1}) \pi_{t-1}(V_t^p = j \mid T_{t-1}) \\ &= \pi_{t-1}(T_{t-1}) \boldsymbol{\varphi}_j(A_t^p).\end{aligned}$$

Hence, we obtain the expression of the marginal distribution of T_t as

$$\begin{aligned}\pi_t(T_t) &= \sum_{i=1}^{I} \sum_{j=1}^{I} \pi_t(T_t, V_t^p = j, V_t = i) \\ &= \frac{Z_t}{Z_{t-1}} \pi_{t-1}(T_{t-1}) P(J_t) \sum_{i=1}^{I} \left\{ \sum_{j=1}^{I} \boldsymbol{\varphi}_j(A_t^p) \boldsymbol{\xi}_{j,i}(A_t) \right\} M_i(A_t \mid J_t) \frac{\mu(\mathbf{x}(A_{t,l}) \mid A_{t,l}) \mu(\mathbf{x}(A_{t,r}) \mid A_{t,r})}{\mu(\mathbf{x}(A_t) \mid A_t)},\end{aligned}$$

which completes the proof. □

Proof of Proposition 3.2

In this discussion, we suppress $\mathbf{x}$ and T^m in the expectation for simplicity. First, when $A = \Omega$, by the definition $e_\Omega(i) = \tilde{\boldsymbol{\gamma}}_{1,i}(\Omega)$. Next, if A is not the root node, we can decompose $e_A(i')$ as

$$e_A(i') = \sum_{i=1}^{I} \mathbb{E}[Q(A) I[V(A) = i'] I[V(A^p) = i]].$$

For the summand, because $\theta(A^p)$ and $V(A)$ are conditionally independent given $V(A^p)$, we obtain

$$\begin{aligned}
&\mathbb{E}[Q(A)I[V(A)=i']I[V(A^p)=i]] \\
&= \mathbb{E}[\mathbb{E}[\vartheta(A^p)I[V(A)=i'] \mid V(A^p)]I[V(A^p)=i]Q(A^p)] \\
&= \mathbb{E}[\mathbb{E}[\vartheta(A^p)I[V(A)=i'] \mid V(A^p)=i]I[V(A^p)=i]Q(A^p)] \\
&= \mathbb{E}[\mathbb{E}[\vartheta(A^p) \mid V(A^p)=i]P(V(A)=i' \mid V(A^p)=i)I[V(A^p)=i]Q(A^p)] \\
&= \tilde{\boldsymbol{\xi}}_{i,i'}\mathbb{E}[\vartheta(A^p) \mid V(A^p)=i]e_{A^p}(i).
\end{aligned}$$

Therefore, we obtain

$$e_A(i') = \sum_{i=1}^{I} \tilde{\boldsymbol{\xi}}_{i,i'}(A)\mathbb{E}[\vartheta(A^p) \mid V(A^p)=i]e_{A^p}(i).$$

Proof of Proposition 4.1

We prove Proposition 4.1 based the following lemma.

Lemma C.2. *For $T \in \mathcal{T}^K$ and $A \in \mathcal{N}(T)$, if $i \in \tau(A \mid T)$, then*

$$\frac{\log M_A(i \mid j_A)}{n} \xrightarrow{p} \sum_{g=1}^{G} \zeta_g P_g(A)\left[P_g(A_l \mid A)\log P_g(A_l \mid A) + P_g(A_r \mid A)\log P_g(A_r \mid A)\right].$$

(Proof) By the result of Schwarz et al. (1978), since the parameter $\theta(A)$ follow the beta distribution, which belongs to a continuous exponential family, the log of the marginal likelihood is written as

$$\begin{aligned}
\log M_A(i \mid T) &= \hat{l}_A(i,T) - \frac{r_i}{2}\log n(A) + \mathcal{O}_p(1), \\
\hat{l}_A(i,T) &= \log\left[\prod_{g=1}^{G} \hat{\theta}_g(A)^{n_g(A_l)}(1-\hat{\theta}_g(A))^{n_g(A_r)}\right] \\
&= \sum_{g=1}^{G}\left[n_g(A_l)\log\hat{\theta}_g(A) + n_g(A_r)\log(1-\hat{\theta}_g(A))\right],
\end{aligned} \tag{20}$$

where the definition of $\hat{\theta}_g(A)$ (the MLE) and r_i (the number of parameters) depend on which type of priors in Assumption 1 is introduced by the state i:

$$\hat{\theta}_g(A) = \begin{cases} \frac{n_g(A_l)}{n_g(A)} & \text{(Prior A)}, \\ \frac{n(A_l)}{n(A)} & \text{(Prior B)}, \\ \frac{\mu(A_l)}{\mu(A)} & \text{(Prior C)}, \end{cases} \quad r_i = \begin{cases} G & \text{(Prior A)}, \\ 1 & \text{(Prior B)}, \\ 0 & \text{(Prior C)}. \end{cases} \tag{21}$$

Since $i \in \tau(A \mid T)$, the law of large numbers gives $\hat{\theta}_g(A) \xrightarrow{p} P_g(A_l \mid A)$. Hence, we obtain the limit of $\hat{l}_A(i,T)/n$ as

$$\begin{aligned}\frac{\hat{l}_A(i,T)}{n} &= \sum_{g=1}^{G} \frac{n_g(\Omega)}{n(\Omega)} \frac{n_g(A)}{n_g(\Omega)} \left[\frac{n_g(A_l)}{n_g(A)} \log \hat{\theta}_g(A) + \frac{n_g(A_r)}{n_g(A)} \log(1 - \hat{\theta}_g(A)) \right] \\ &\xrightarrow{p} \sum_{g=1}^{G} \zeta_g P_g(A) \left[P_g(A_l \mid A) \log P_g(A_l \mid A) + P_g(A_r \mid A) \log P_g(A_r \mid A) \right].\end{aligned}$$

□

(Proof of Proposition 4.1) The ratio of the density functions is rewritten as

$$\frac{\mu(\mathbf{x}(A_l) \mid A_l)\mu(\mathbf{x}(A_r) \mid A_r)}{\mu(\mathbf{x}(A) \mid A)} = \mu(A_l \mid A)^{-n(A_l)} \mu(A_r \mid A)^{-n(A_r)}.$$

Hence we obtain

$$\begin{aligned}&\log \left(\frac{\mu(\mathbf{x}(A_l) \mid A_l)\mu(\mathbf{x}(A_r) \mid A_r)}{\mu(\mathbf{x}(A) \mid A)} \right) \Big/ n \\ &= -\frac{n(A_l)}{n} \log \mu(A_l \mid A) - \frac{n(A_r)}{n} \log \mu(A_r \mid A) \\ &\xrightarrow{p} -\sum_{g=1}^{G} \zeta_g \left\{ P_g(A_l) \log \mu(A_l \mid A) + P_g(A_r) \log \mu(A_r \mid A) \right\} \\ &= -\sum_{g=1}^{G} \zeta_g P_g(A) \left\{ P_g(A_l \mid A) \log \mu(A_l \mid A) + P_g(A_r \mid A) \log \mu(A_r \mid A) \right\}.\end{aligned}$$

This result and Lemma C.2 give the limit in (13). □

Proof of Theorem 4.1 and Theorem 4.2

In this proof, we modify the notation for the marginal likelihood defined in Eq. (5) and use $M_A(i \mid T)$ to represent the likelihood on A of the tree T under the ith state to reflect its dependency on the tree structure.

We first prove a lemma on the marginal likelihoods under different states.

Lemma C.3. *For $T \in \mathcal{T}^K$, $A \in \mathcal{N}(T)$, $i \in \tau(A \mid T)$ and $j \in \{1, \ldots, I\}$, we have*

$$\frac{\log M_A(i \mid T) - \log M_A(j \mid T)}{n} \xrightarrow{p} c_{i,j},$$

where $c_{i,j} = 0$ if $j \in \tau(A \mid T)$ and $c_{i,j} > 0$ if $j \in \{1, \ldots, I\} \setminus \tau(A \mid T)$.

(Proof) If $j \in \tau(A \mid T)$, obtaining the result

$$\frac{\log M_A(i \mid T) - \log M_A(j \mid T)}{n} \xrightarrow{p} 0$$

is straightforward from the proof of Proposition C.2. Hence we consider the case of $j \in \{1, \ldots, I\} \setminus \tau(A \mid T)$. Under the state j, for every g, the estimator $\hat{\theta}_g(A)$ is defined as in (21), and there exists $B_g \in (0, 1)$ such that $\hat{\theta}_g(A) \xrightarrow{p} B_g$. By the definition of $\tau(A \mid T)$, there exists g^* such that $B_{g^*} \neq P_{g^*}(A_l \mid A)$. As in the proof of Proposition C.2, for the difference of the marginal likelihoods, we obtain

$$\frac{\log M_A(i \mid T) - \log M_A(j \mid T)}{n} \xrightarrow{p} \sum_{g=1}^{G} \zeta_g P_g(A) \Lambda_g,$$

$$\Lambda_g = P_g(A_l \mid A) \log \frac{P_g(A_l \mid A)}{B_g} + P_g(A_r \mid A) \log \frac{P_g(A_r \mid A)}{1 - B_g}.$$

Because Λ_g is the KL divergence of the two discrete distributions, $\Lambda_g \geq 0$ for all g and $\Lambda_{g^*} > 0$. By Assumption 1, this result implies that

$$\sum_{g=1}^{G} \zeta_g P_g(A) \Lambda_g > 0.$$

□

(Proof of Theorem 4.1 and Theorem 4.2)

Let $T \in \mathcal{T}^K$ and $\mathcal{V}$ denote a set of a combination of the states for all of the non-leaf nodes of T. Notice that an element of $\mathbf{V}$ does not need to satisfy $P(\mathbf{V} = \mathbf{v}) > 0$, where $\mathbf{V}$ is the totality of the state variables. In the following proof, for $\mathbf{v} \in \mathcal{V}$, $\mathbf{v}(A)$ denotes a state on a node A. Let $l(\mathbf{v}, T)$ denote the log of the joint likelihood function

$$l(\mathbf{v}, T) = \log P(\mathbf{x}_n \mid T, \mathbf{v}) = \sum_{A \in \mathcal{N}(T)} l_A(\mathbf{v}(A), T) + \sum_{A \in \mathcal{L}(T)} \log \mu(\mathbf{x}_n(A) \mid A), \tag{22}$$

where $l_A(\mathbf{v}(A), T) = \log M_A(\mathbf{v}(A) \mid T)$. By Schwarz et al. (1978), this likelihood l_A has the following expression

$$l_A(\mathbf{v}(A), T) = \hat{l}_A(\mathbf{v}(A), T) - \frac{r_{\mathbf{v}(A)}}{2} \log n(A) + \mathcal{O}_p(1),$$

where $\hat{l}_A$ and r_i are defined in (20). Let $\bar{\mathbf{v}} \in \mathcal{V}$ be a collection of states such that, for all $A \in \mathcal{N}(T)$, $\theta_g(A)$ is fixed to $\mu(A_l)/\mu(A)$. For $\bar{\mathbf{v}}$, we have

$$\begin{aligned} l_A(\bar{\mathbf{v}}, T) &= \sum_{A \in \mathcal{N}(T)} \left\{ n(A_l) \log \left(\frac{\mu(A_l)}{\mu(A)} \right) + n(A_r) \log \left(\frac{\mu(A_r)}{\mu(A)} \right) \right\} + \sum_{A \in \mathcal{L}(T)} \log \mu(\mathbf{x}_n(A) \mid A) \\ &= \log \mu(\mathbf{x}) = 0. \end{aligned}$$

Hence $l(\mathbf{v}, T)$ is rewritten as

$$l(\mathbf{v}, T) = l(\mathbf{v}, T) - l(\bar{\mathbf{v}}, T) = \sum_{A \in \mathcal{N}(T)} \left\{ \hat{l}_A(\mathbf{v}(A), T) - \hat{l}_A(\bar{\mathbf{v}}(A), T) \right\} - \frac{C(\mathbf{v})}{2} \log n + \mathcal{O}_p(1).$$

For the part inside of the braces, when $\mathbf{v}$ is replaced with $\mathbf{v}_T \in \mathcal{V}_T$, where $\mathcal{V}_T = \{\mathbf{v} : \mathbf{v}(A) \in \tau(A \mid T) \text{ for all } A \in \mathcal{N}(T)\}$, the definition of $\hat{l}_A$ gives

$$\begin{aligned}
\frac{\hat{l}(\mathbf{v}_T(A), T) - \hat{l}(\bar{\mathbf{v}}(A), T)}{n} &= \sum_{g=1}^{G} \frac{n_g(A)}{n} \left[\frac{n_g(A_l)}{n_g(A)} \log \frac{\hat{\theta}_g(A)}{\mu(A_l \mid A)} + \frac{n_g(A_r)}{n_g(A)} \log \frac{1 - \hat{\theta}_g(A)}{\mu(A_r \mid A)} \right] \\
&\xrightarrow{p} \sum_{g=1}^{G} \zeta_g P_g(A) \left[P_g(A_l \mid A) \log \frac{P_g(A_l \mid A)}{\mu(A_l \mid A)} + P_g(A_r \mid A) \log \frac{P_g(A_r \mid A)}{\mu(A_r \mid A)} \right].
\end{aligned}$$

For all $A \in \mathcal{L}(T)$, there exists an unique sequence of nodes

$$\Omega = B_{A,0} \supset B_{A,1} \supset \cdots \supset B_{A,K} = A, \tag{23}$$

where $B_{A,k} \in T$ $(k = 0, \ldots, K)$ is a node in the kth level. With this sequence, we obtain the limit of the scaled log-likelihood as

$$\begin{aligned}
&\frac{l(\mathbf{v}_T, T)}{n} \\
&\xrightarrow{p} \sum_{A \in \mathcal{N}(T)} \sum_{g=1}^{G} \zeta_g P_g(A) \left[P_g(A_l \mid A) \log \frac{P_g(A_l \mid A)}{\mu(A_l \mid A)} + P_g(A_r \mid A) \log \frac{P_g(A_r \mid A)}{\mu(A_r \mid A)} \right] \\
&= \sum_{g=1}^{G} \zeta_g \sum_{A \in \mathcal{N}(T)} \left[P_g(A_l) \log \frac{P_g(A_l \mid A)}{\mu(A_l \mid A)} + P_g(A_r) \log \frac{P_g(A_r \mid A)}{\mu(A_r \mid A)} \right] \\
&= \sum_{g=1}^{G} \zeta_g \sum_{A \in \mathcal{L}(T)} P_g(A) \left[\log \frac{P_g(B_{A,1} \mid B_{A,0})}{\mu(B_{A,1} \mid B_{A,0})} + \cdots + \log \frac{P_g(B_{A,K} \mid B_{A,K-1})}{\mu(B_{A,K} \mid B_{A,K-1})} \right] \\
&= \sum_{g=1}^{G} \zeta_g \sum_{A \in \mathcal{L}(T)} P_g(A) \log \frac{P_g(A)}{\mu(A)} = \sum_{g=1}^{G} \zeta_g KL(P_g|_T || \mu).
\end{aligned} \tag{24}$$

Because $P_g|_T$ admits the density function

$$p_g|_T(x) = \sum_{A \in \mathcal{L}(T)} \mathbf{1}_A(x) \frac{P_g(A)}{\mu(A)}, \ x \in \Omega$$

the KL divergence in (24) is rewritten as

$$\begin{aligned}
KL(P_g|_T||\mu) &= \sum_{A\in\mathcal{L}(T)} P_g(A)\log\frac{P_g(A)}{\mu(A)} \\
&= \int p_g \sum_{A\in\mathcal{L}(T)} \mathbf{1}_A \log\frac{P_g(A)}{\mu(A)} d\mu \\
&= \int p_g \log p_g|_T d\mu \\
&= \int p_g(x)\log\frac{p_g(x)}{\mu(x)} d\mu(x) - \int p_g \log\frac{p_g}{p_g|_T} d\mu \\
&= KL(P_g||\mu) - KL(P_g||P_g|_T).
\end{aligned}$$

Because $KL(P_g||\mu)$ is independent of T, we obtain another expression of $\mathcal{T}_M^K$ in (14) as

$$\mathcal{T}_M^K = \arg\max_{T\in\mathcal{T}^K} \sum_{g=1}^{G} \zeta_g KL(P_g|_T||\mu)$$

By Lemma C.3 and (22), for $\mathbf{v}\in\mathcal{V}\setminus\mathcal{V}_T$, we can show that

$$\text{p-lim}_{n\to\infty} \frac{l(\mathbf{v},T)-l(\mathbf{v}_T,T)}{n} = \text{p-lim}_{n\to\infty} \sum_{A\in\mathcal{N}(T)} \frac{l_A(\mathbf{v},T)-l_A(\mathbf{v}_T,T)}{n} > 0, \tag{25}$$

and $\text{p-lim}_{n\to\infty} l(\mathbf{v},T)/n$ exists. Hence, for $T_M\in\mathcal{T}_M^K$, $\mathbf{v}'\in\mathcal{V}_{T_M}$, $T\in\mathcal{T}^K\setminus\mathcal{T}_M^K$ and $\mathbf{v}\in\mathcal{V}$, we have

$$\text{p-lim}_{n\to\infty} \frac{l(\mathbf{v}',T_M)-l(\mathbf{v},T)}{n} \geq \sum_{g=1}^{G}\zeta_g KL(P_g|_{T_M}||\mu) - \sum_{g=1}^{G}\zeta_g KL(P_g|_T||\mu) > 0.$$

Therefore for such $\mathcal{T}_M$ and $\mathbf{v}'$, we obtain

$$\frac{P(\mathbf{x}_n \mid T)}{P(\mathbf{x}_n \mid T_M)} = \frac{\sum_{\mathbf{v}\in\mathcal{V}}\exp(l(\mathbf{v},T))P(\mathbf{v})}{\sum_{\mathbf{v}\in\mathcal{V}}\exp(l(\mathbf{v},T_M))P(\mathbf{v})} \leq \sum_{\mathbf{v}\in\mathcal{V}} \frac{\exp(l(\mathbf{v},T))P(\mathbf{v})}{\exp(l(\mathbf{v}',T_M))P(\mathbf{v}')} \xrightarrow{p} 0.$$

This result implies $p(T\in\mathcal{T}_M^K \mid \mathbf{x}_n)\xrightarrow{p} 1$, which completes the proof of Theorem 4.1.

To prove Theorem 4.2, we fix $T\in\mathcal{T}^K$ and define a set $\mathcal{S}_T$ as

$$\mathcal{S}_T = \left\{\mathbf{v}\in\mathcal{V}_T \mid \mathbf{v}\in\arg\min_{\mathbf{v}'\in\mathcal{V}_T} C(\mathbf{v}')\right\}.$$

Then we want to show $P(\mathbf{V}\in\mathcal{S}_T \mid T,\mathbf{x}_n)\xrightarrow{p} 1$. The result (25) implies

$$p(\mathbf{V}\in\mathcal{V}_T \mid T,\mathbf{x}_n)\xrightarrow{p} 1,$$

so we only need to compare the elements of $\mathcal{V}_T$. Let $\mathbf{v} \in \mathcal{V}_T \backslash \mathcal{S}_T$ and $\mathbf{v}' \in \mathcal{S}_T$. For the difference of the log likelihoods, we have

$$l(\mathbf{v}', T) - l(\mathbf{v}, T) = \sum_{A \in \mathcal{N}(T)} \left[\hat{l}_A(\mathbf{v}'(A), T) - \hat{l}_A(\mathbf{v}(A), T) \right] + \frac{C(\mathbf{v}) - C(\mathbf{v}')}{2} \log n + \mathcal{O}_p(1),$$

where $\hat{l}_A$ and C is defined in (21) and (15), respectively. If $\mathbf{v}(A)$ and $\mathbf{v}'(A)$ introduce the same type of the prior (e.g., Prior A and Prior A), because the corresponding estimators $\hat{\theta}_g(A)$ have the same form,

$$\hat{l}_A(\mathbf{v}'(A), T) - \hat{l}_A(\mathbf{v}(A), T) = 0.$$

On the other hand, if $\mathbf{v}(A)$ and $\mathbf{v}'(A)$ introduce different types of the prior (e.g., Prior A and Prior B), because they are the maximized log-likelihood under the two nested hypotheses,

$$-2[\hat{l}_A(\mathbf{v}'(A), T) - \hat{l}_A(\mathbf{v}(A), T)]$$

weakly converges to the χ^2 distribution (Wilks, 1938). Hence, we obtain

$$\frac{l(\mathbf{v}', T) - l(\mathbf{v}, T)}{\log n} \xrightarrow{p} \frac{C(\mathbf{v}) - C(\mathbf{v}')}{2} > 0,$$

which implies $P(\mathbf{V} \in \mathcal{S}_T \mid T, \mathbf{x}_n) \xrightarrow{p} 1$. □

D Consistency for the MRS model

To describe the consistency, for a possible node A, we define a variable $Z(A)$ as follows:

$$Z(A) = \begin{cases} 1 & \text{if } V(A) = 1, \\ 0 & \text{if } V(A) \in \{2, 3\}. \end{cases}$$

Hence, $\theta_1(A) = \theta_2(A)$ if $Z(A) = 0$ and $\theta_1(A) \neq \theta_2(A)$ with probability one if $Z(A) = 1$. Then we can obtain the following consistency result.

Corollary D.1. *Let $\mathbf{Z} = \{\mathbf{Z}(A)\}_{A \in \mathcal{N}(T)}$ and $\mathbf{z} = \{\mathbf{z}(A)\}_{A \in \mathcal{N}(T)}$ be a collection of $Z(A)$ on $T \in \mathcal{T}^K$ and one of its realizations, respectively. If $P(\mathbf{Z} = \mathbf{z}) > 0$ for any possible $\mathbf{z}$, then*

$$P\left(Z(A) = \mathbf{1}_{\{P_1(A_l|A) \neq P_2(A_l|A)\}} \text{ for all } A \in \mathcal{N}(T) \mid T, \mathbf{x}_n\right) \xrightarrow{p} 1,$$

where $\mathbf{1}$ is the indicator function, and

$$P\left(Z(A) = \mathbf{1}_{\{P_1(A_l|A) \neq P_2(A_l|A)\}} \text{ for all } A \in \mathcal{N}(T) \mid \mathbf{x}_n\right) \xrightarrow{p} 1,$$

where T is random.

(Proof) In this case, $\mathcal{V}_T$ in Theorem 4.2 is written as

$$\mathcal{V}_T = \{\mathbf{v} \mid \mathbf{v}(A) = 1 \text{ if } P_1(A_l \mid A) \neq P_2(A_l \mid A)\}.$$

We additionally define $\tilde{\mathcal{V}}_T$ as

$$\tilde{\mathcal{V}}_T = \{\mathbf{v} \mid \mathbf{v}(A) = 2 \text{ if } P_1(A_l \mid A) = P_2(A_l \mid A)\}.$$

Then, under the condition that $\mathbf{v} \in \mathcal{V}_T$, the complexity $C(\mathbf{v})$ is minimized if and only if $\mathbf{v} \in \tilde{\mathcal{V}}_T$. Hence, by Theorem 4.2 we obtain

$$\begin{aligned} &P\left(Z(A) = \mathbf{1}_{\{P_1(A_l|A) \neq P_2(A_l|A)\}} \text{ for all } A \in \mathcal{N}(T) \mid T, \mathbf{x}_n\right) \\ &= P\left(\mathbf{V} \in \mathcal{V}_T \cap \tilde{\mathcal{V}}_T \mid T, \mathbf{x}_n\right) \xrightarrow{p} 1. \end{aligned}$$

We can show the second result by using Theorem 4.1 as follows:

$$\begin{aligned} P\left(\mathbf{V} \in \mathcal{V}_T \cap \tilde{\mathcal{V}}_T \mid \mathbf{x}_n\right) &= \sum_{T \in \mathcal{T}^K} P\left(\mathbf{V} \in \mathcal{V}_T \cap \tilde{\mathcal{V}}_T \mid T, \mathbf{x}_n\right) P(T \mid \mathbf{x}_n) \\ &\geq \arg\min_{T_M \in \mathcal{T}_M^K} P\left(\mathbf{V} \in \mathcal{V}_T \cap \tilde{\mathcal{V}}_T \mid T_M, \mathbf{x}_n\right) P(T \in \mathcal{T}_M^K \mid \mathbf{x}_n) \\ &\xrightarrow{p} 1. \end{aligned}$$

□